

KfK 4297

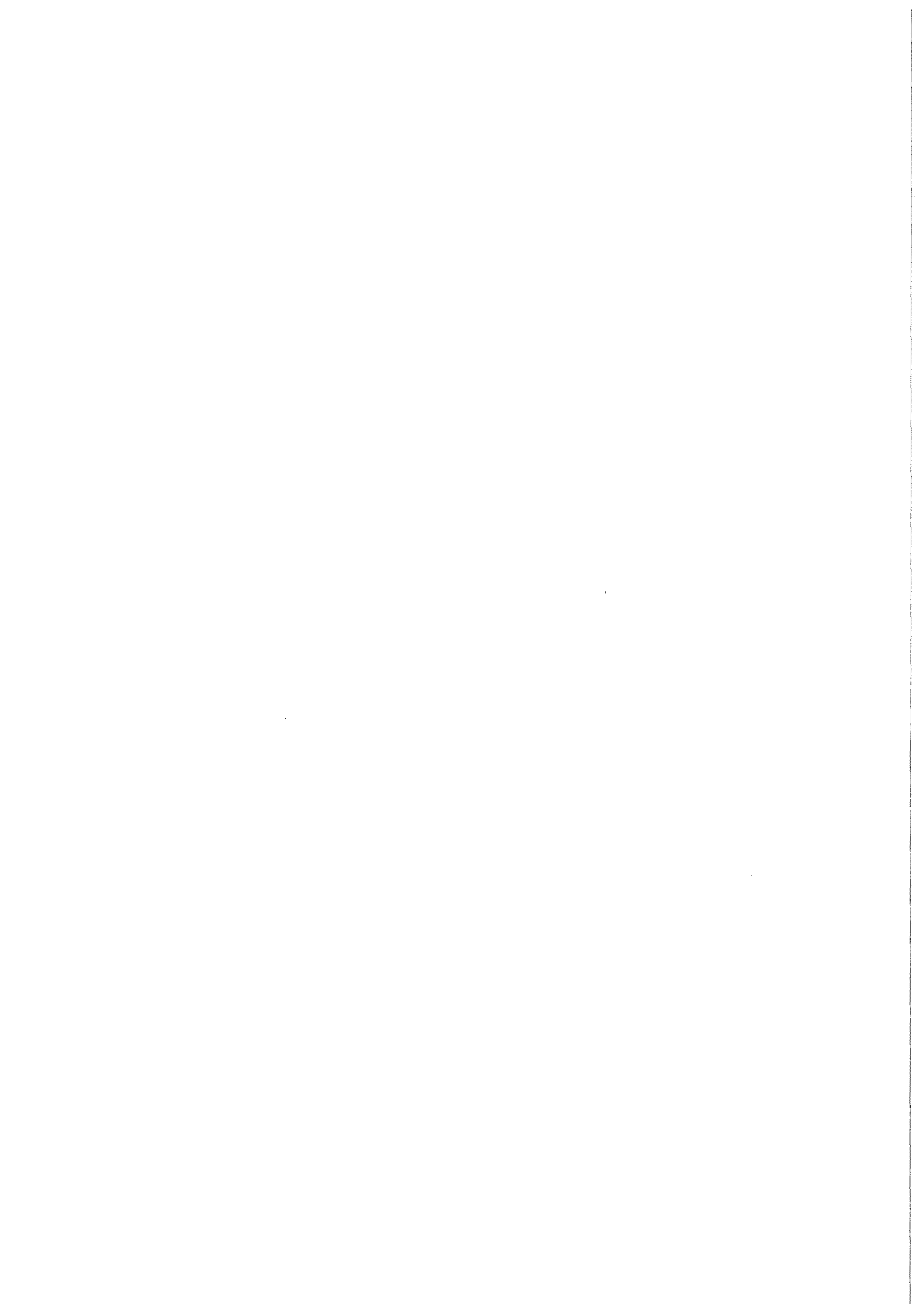
Juli 1988

XPS and AES Investigations of the Adhesive Bonding Properties of Thin Titanium Coatings

H. Moers, J. Mohr, H. Klewe-Nebenius, G. Pfennig

Institut für Radiochemie
Institut für Kernverfahrenstechnik

Kernforschungszentrum Karlsruhe



KERNFORSCHUNGSZENTRUM KARLSRUHE

Institut für Radiochemie
Institut für Kernverfahrenstechnik

KfK 4297

XPS and AES Investigations of the Adhesive Bonding
Properties of Thin Titanium Coatings

H. Moers*, J. Mohr, H. Klewe-Nebenius and G. Pfennig

*Present address: Hoechst AG, Werk Kalle
P.O. Box 35 40
D-6200 Wiesbaden 1, F.R.G.

KERNFORSCHUNGSZENTRUM KARLSRUHE GMBH, KARLSRUHE

Als Manuskript vervielfältigt
Für diesen Bericht behalten wir uns alle Rechte vor

Kernforschungszentrum Karlsruhe GmbH
Postfach 3640, 7500 Karlsruhe 1

ISSN 0303-4003

Abstract

The bonding properties of PMMA-microstructures on Ti-coated Cu-substrates after an oxidative treatment in alkaline hydrogenperoxide solution were investigated. In order to clarify the basic mechanism, surface analytical investigations by XPS-, AES-, and depth profile measurements have been performed. It was demonstrated that for optimum bonding a TiO₂ surface layer of ca. 30 nm thickness is necessary. Chemical effects as well as a mechanical bonding with open grain boundary structures (dimensions in the µm-range) could be ruled out as bonding mechanisms. A mechanical interlocking of the polymer with micropores (dimensions in the nm-range) of the oxidic overlayer is adopted as the most probable bonding mechanism.

XPS und AES Untersuchungen zur Hafteigenschaft dünner Titanschichten

Zusammenfassung

Die Hafteigenschaften von PMMA-Mikrostrukturen auf Titan-beschichteten Kupferträgern nach einer Ätzbehandlung in alkalischer Wasserstoffperoxid-Lösung wurden untersucht. Zur Aufklärung des zugrunde liegenden Mechanismus wurden oberflächenanalytische Untersuchungen mit XPS- AES- und Tiefenprofilmessungen durchgeführt. Es konnte gezeigt werden, daß zur optimalen Haftung eine oberflächliche TiO₂-Schicht von ca. 30 nm Dicke erforderlich ist. Als Mechanismen für die Haftung konnten chemische Effekte sowie eine mechanische Verzahnung mit offenen Korngrenzenstrukturen (Dimensionen im µm-Bereich) ausgeschlossen werden. Als wahrscheinlichster Haftmechanismus wird eine Verzahnung des Polymers mit Mikroporen der oxidischen Deckschicht (Dimensionen im nm-Bereich) angenommen.

Contents

	Page
1. Introduction	1
2. Experimental	3
2.1 Substrates	3
2.2 Oxidation Procedure	3
2.3 Measurements	4
2.4 Testing of Bonding Properties	6
3. Results and Discussion	6
3.1 Characterization of Untreated Ti/Cu samples	6
3.1.1 Metallographic characterization	6
3.1.2 Surface analytical characterization	7
3.2 Effects of Oxidative Treatment	8
3.2.1 Weight loss and X-ray fluorescence absorption measurements	9
3.2.2 Roughness and topography change measurements	9
3.2.3 Results of XPS and AES measurements	10
3.2.4 Results on bonding properties	12
3.3 Correlation of Surface Analyses and Bonding Properties	13
4. Summary	14
5. References	16
Table 1	18
Figures	20

1. Introduction

The investigation of bonding and adhesion properties of various kinds of materials has attained increasing significance for numerous technological applications. Besides the creation of durable junctions between equal as well as different materials the ample field of coatings depends widely on information on the adhesion properties of the materials involved.

Examples, where such questions arise, are hard coatings for the improvement of wear properties or paint coatings for corrosion protection purposes. Furthermore, during the fabrication of semiconductors thin coatings of photosensitive polymeric material are used as masks for the structurization of thin films on top of an appropriate substrate, e.g. silicon (1). Several hundred μm thick polymeric coatings on metallic substrates are used in the fabrication of microstructures with high aspect ratio by the so-called LIGA process (2-4). This procedure has been developed at the Kernforschungszentrum Karlsruhe and consists of a sequence of several steps: irradiation and development of the polymeric coating, galvanofarming, mould fabrication, and replication by reaction injection moulding. During the irradiation step an X-ray sensitive polymer (polymethylmethacrylate, PMMA) of several hundred micrometers thickness, which has been directly polymerized on top of an appropriate metallic base plate, is irradiated with synchrotron radiation through a mask. After development of the irradiated parts of the polymer the cavities are refilled by galvanic metal precipitation. After removal of the residual polymer, this metallic form is used for the replication of the microstructures in a mass production process.

For the performance of the lithographic and subsequent steps of the LIGA process it is important to achieve an optimum junction between the polymer and the support which can withstand mechanical and chemical stresses. Even microstructures with dimensions down to a few micrometers must adhere after development.

There exist numerous investigations which deal with the adhesion and bonding properties of various materials and which concern the effects of chemical and/or mechanical pretreatments of the solid materials (e.g. metals) which are to be bonded to their counterpart or which serve as support for a polymer (5-11). The aim of these works was to find the optimum pretreatment conditions for bonding and to determine what properties of the pretreated substrate are responsible for a good bonding.

It is common use to subdivide the adhesion properties into those which are based on mechanical reasons and those which are affected by chemical interactions (5,12). In case of "mechanical" adhesion the interaction between the adhesive and the adherend can be described by a mechanical interlocking between the porous surface of the adherend and the adhesive, which is able to penetrate into the pores before solidification (5-7).

Chemical interactions are based on the formation of chemical bonds between the two adjacent solids. Another possibility is the existence of a diffusion zone which is characterized by a high degree of interdiffusion and the presence of solid solutions of wide homogeneity range or of multiphase systems (13-16).

Much of the discussion concerns the degree of mechanical or chemical interactions contributing to the bonding strengths. It seems that in metal/polymer systems mechanical interlocking is the dominating process. However, it cannot be ruled out that chemical bonding contributes to the stability of the junction, too (5).

The aim of the present work is to elucidate the results of experimental investigations which describe the bonding properties of PMMA on titanium coated copper base plates, which are used during the structurization steps of the LIGA process. Before use the Ti/Cu base plates are treated with an alkaline hydrogen peroxide solution. This treatment has been shown to improve the bonding properties of titanium and titanium based alloys to a high extent (8,17). In case of PMMA as polymeric overlayer it has been observed that the adhesion of the microstructure depends strongly on the time of oxidative pretreatment of the support.

Surface analytical techniques and among these XPS and AES provide information from a surface layer of only a few nanometers thickness and are, therefore, well suited for the investigation of possible chemical effects on the adhesion properties and on the long-term resistance of metal-to-polymer junctions since these effects should occur primarily at the interface between both solids (5-7,9,10,14-16,18-20).

Since the Ti-coating has only a thickness of up to a few micrometers, besides a functional testing depth profiling by combining Auger Electron Spectroscopy (AES) with ion bombardment induced sputtering has been used for the investigation of the compositional changes of the coating caused by the etching treatment.

2. Experimental

2.1 Substrates

The substrates used as base plates for the PMMA resist in deep-etch X-ray lithography consist of copper plates of about 2 mm thickness, which are coated with a titanium layer of a few micrometers thickness. Before coating the copper plates are milled on one side with a fast-running milling machine to obtain a smooth surface. Afterwards the plates are coated on this side with a one to three micrometer thick titanium overlayer by sputter deposition.

Sputtering of the Ti-layers has been done using a magnetron sputtering apparatus type Z 700P1 (Leybold-Heraeus), allowing a residual gas pressure of down to 8×10^{-8} mbar. Two types of coatings have been produced depending on the sputtering conditions (21,22): Ti-layers with open grain boundaries have been obtained by applying a high argon process pressure of 3×10^{-2} mbar, a low substrate bias voltage of -40 V, an average deposition rate of $20 \text{ \AA}/\text{sec}$ and an average substrate temperature of $200 \text{ }^\circ\text{C}$. Overlayers with closed grain boundaries and accordingly mirrorlike surfaces have been obtained primarily by lowering the gas pressure during sputtering to 4×10^{-3} mbar and by increasing the bias voltage to -100 V. The appearance or absence of open grain boundaries in dependence on the sputtering conditions can be explained by the Thornton model (23). In the present work both types of coatings have been investigated.

2.2 Oxidation Procedure

The Ti/Cu samples were oxidized in an alkaline hydrogen peroxide solution (0.5 M NaOH, 0.2 M H_2O_2) (17). The reaction temperature was kept constant at $65 \pm 1 \text{ }^\circ\text{C}$. The oxidation time was varied between one and twenty minutes. The solution was permanently mixed by a magnetic stirrer running with a frequency of 250 cycles per minute.

During the experiments it turned out to be necessary to control the experimental conditions very carefully since otherwise differences in the degree of oxidative attack were observed, especially for samples with open grain boundaries in the Ti-coating. The following conditions had to be maintained in order to obtain reproducible results of the oxidative treatment:

- addition of the H_2O_2 -solution before heating,
- heat-up time of the $H_2O_2/NaOH$ solution before sample insertion about 30 min,
- constant mixing speed,
- sufficient volume of the etch solution in order to keep its consumption negligible during etching (0.5 l of $H_2O_2/NaOH$ solution for samples with a coated area of $60 \times 15 \text{ mm}^2$),
- use of a fresh solution for each etch treatment.

2.3 Measurements

The absorption of X-ray fluorescence radiation from the Cu-substrate in the Ti-coating was used to determine the thickness decrease of the coating caused by the oxidative treatment. With this technique the thickness of an overlayer is calculated from the intensity of secondary X-rays emitted from the substrate, which is proportional to the overlayer thickness (24). Since this is only an indirect method, the intensity scale has to be calibrated using a layer of known thickness. This has been done by measuring the step height of a titanium layer covering the Cu-substrate only partially by means of a step profiler. In addition, some samples were weighed before and after oxidation. The weight loss was then transformed into the degree of reduction of overlayer thickness. This latter method was also used to prove that copper was not attacked significantly by the peroxide solution. This is of importance because only one side of the copper plates was covered with titanium.

Topographical as well as structural changes of the overlayer after oxidation were examined in a scanning electron microscope. For this purpose the titanium surface of the oxidized samples and, in addition, cross-sections perpendicular to the surface were investigated. The latter were made by etching a window into the Cu-base plate with a solution of 30 % HNO_3 which does not attack the Ti-overlayer. The self-supporting Ti-foil of one to three μm thickness was then broken mechanically.

The roughness of the surface was determined by means of a "step-profiler" from a cross-surface plot obtained from the vertical deflections of the diamond-tipped stylus, which is moved across the sample surface. The stylus used had a tip radius of less than $1 \mu\text{m}$. This means that e.g. the depth of $1 \mu\text{m}$ diameter holes could only be measured if it is less than $1/8$ of the diameter. Parameters to characterize the

roughness are the maximum height of the surface roughness R_T and the root mean square deviation from the average surface roughness R_a , which were determined along a distance of 200 μm .

For the measurement of XPS and AES spectra and of depth profiles 20 x 20 mm^2 squares of all sample types were stuck to standard probes by means of adhesive silver paint, which was allowed to dry in atmosphere under ambient conditions or sometimes by using an infra-red lamp. Afterwards the samples were introduced into the spectrometer.

The spectrometer used was a Vacuum Generators (VG) ESCALAB 5 which is described in detail elsewhere (25). XPS spectra were recorded with Al K X-ray excitation with the energy analyzer operated in the constant pass energy mode (CAE). Overview spectra were recorded with CAE = 50 eV while narrow scans around the energies of the important electron lines were taken with CAE = 20 eV. With the latter value the resolution of the spectrometer has been determined to be 1.3 eV (FWHM) for the Au 4f photopeaks of a cleaned gold sample. Binding energies are referred to the Au 4f_{7/2} photopeak with $E_B = 84.0$ eV. The XPS spectra represent the average composition of a sample surface of 50 mm^2 area.

Auger electron emission was excited by 3 or 5 keV primary electrons from a VG LEG 100 electron gun with a focussed beam of 1-3 μm diameter which was usually rastered over a sample area of 0.24 mm^2 . The total electron current amounted to 2.0 μA . During the acquisition of AES spectra the electron spectrometer was operated in the constant retard ratio mode (CRR) with a value of CRR = 10. Spectra were recorded in the derivative mode by using a lock-in amplifier and a modulation voltage of 2.0 V. Elemental intensities were determined from the peak-to-peak heights of the differentiated Auger lines.

The surface erosion for the measurement of depth distributions was performed with 5 keV Ar ions using a VG AG 61 ion gun which provides a focussed (ca. 100 μm ϕ) and rastered ion beam. The total ion current was chosen between 100 and 500 nA, and the ion current densities ranged from 25 to 500 $\text{nA} \cdot \text{mm}^{-2}$. No influence of a variation of the ion current density on the depth profiles could be observed during the measurements. All depth profiles shown in the following are normalized in such a way that the time axis corresponds to constant sputtering conditions of 5 keV Ar⁺ ions at a current density of 200 $\text{nA} \cdot \text{mm}^{-2}$.

For XPS depth profiles the samples were sputtered with argon ions of about 5 keV primary energy from a Leybold-Heraeus IQP 10/63 ion gun. This ion gun provides a homogeneous current density over an area of 10 mm diameter and is, therefore, well suited for a combination with XPS. The current density was about $150 \text{ nA} \cdot \text{mm}^{-2}$.

Data acquisition as well as evaluation and handling of the spectra was performed with a VG DS 4025 data system. Among others it contains routines for the subtraction of X-ray satellites and the background of inelastically scattered electrons, for the determination of peak areas, for the analysis of complex multiplets in XPS spectra by a curve synthesis, and for the evaluation of depth profiles from peak-to-peak heights of AES spectra.

2.4 Testing of Bonding Properties

Testing of the bonding properties of the PMMA microstructures by means of the wedge-test method (26) is not possible due to their small lateral dimensions. Since, however, a correlation of the quality of the bonding properties with the applied oxidation time is necessary, a functional testing was performed.

For this purpose different cylindrical microstructures (diameters 5, 10, 50, 100, 250, and 500 μm , height 100 μm) were produced by deep-etch synchrotron radiation lithography on a single oxidized Ti/Cu sample. The degree of adhesion was characterized by the diameter of the smallest structures, which adhered undisturbed at the surface. In cases where only the smallest microstructures did not adhere completely, the percentage of adhering 5 μm -cylinders was taken as a quantitative measure for the degree of adhesion.

3. Results and Discussion

3.1 Characterization of Untreated Ti/Cu-Samples

3.1.1 Metallographic characterization

The sputtered Ti-layers are different in their optical appearance dependent on the sputtering conditions. Whereas the layers produced without open grain boundaries are brilliant, the surfaces with open grain boundaries look mat. SEM-pictures show that the surfaces of samples without open grain boundaries have a fairly smooth

topography (Fig. 1 a). Their cross-sections are also smooth except of the breaking edges (Fig. 1 b). In contrast, the surfaces of samples with open grain boundaries are distinctly structured (Fig. 2 a). The surfaces are not closed and individual grains are clearly separated from each other. The grooves between the grains extend throughout almost the whole overlayer (Fig. 2 b) and only a thin layer of the coating in contact with the Cu-support is free of open grain boundaries.

As already seen from the SEM-pictures the roughness of surfaces with open grain boundaries is larger than for surfaces without open grain boundaries. This could not completely be reproduced in roughness measurements. The measured parameters for the first sample type are only $R_a = 14$ nm and $R_T = 114$ nm while the values for the latter samples were found to be $R_a = 7$ nm and $R_T = 45$ nm, respectively. The micro-porous structure of the oxide layer is not detectable in these measurements.

3.1.2 Surface analytical characterization

The surfaces of the different unoxidized (and oxidized, see sect. 3.2.3) Ti/Cu samples were characterized by means of XPS and AES. Fig. 3 shows an XPS overview spectrum of sample No. 1 (with open grain boundaries). The surface consists of Ti, O, and C (from adsorbed hydrocarbons). Fig. 4 shows detailed spectra of the Ti 2p and O 1s regions. The Ti 2p spectrum consists of two components, which can be assigned to titanium dioxide and to titanium metal by comparison with published binding energy values (27,29). TiO_2 originating from oxidation during atmospheric contact forms a very thin overlayer of a few nanometers thickness, which protects the underlying metal from further oxidation. The O 1s spectrum is mainly attributed to the dioxide. A contribution of hydroxide at the sample surface is indicated by the asymmetric tailing of the photopeak at its high binding energy side. The XPS spectra of unoxidized samples without open grain boundaries do not differ from those in Figs. 3 and 4.

The AES depth profiles of unoxidized samples with and without open grain boundaries, however, exhibit marked differences with respect to the oxygen depth distribution. Fig. 5 shows the depth profile of sample No. 5 (with open grain boundaries) and Fig. 6 an expansion of the surface-near part of the profile of Fig. 5. In Fig. 7 selected Auger spectra are presented corresponding to various sputtering times of the profile in Fig. 5.

Fig. 8 shows the depth profile of sample No. 9 without open grain boundaries in the Ti-overlayer while an expansion of the surface-near part is given in Fig. 9 and the corresponding selected Auger spectra in Fig. 10.

A comparison of the profiles of samples with and without open grain boundaries (Figs. 5,6 and 8,9) reveals the following features: The oxygen distribution close to the surface is similar in both cases and corresponds, as already observed in XPS spectra, to the coverage of Ti-metal with a thin dioxidic overlayer. The position of the intersection of the Ti(L₃M₂₃M₂₃) and O(KLL) depth profiles (Figs. 6 and 9) can be taken as a measure of the approximate thickness of this overlayer, which can be calculated to be 3 to 4 nm by using a sputtering rate of 2.04 nm/min for TiO₂ at 200 nA/mm² (Ref. 29). However, while in Fig. 8 (sample No. 9, without open grain boundaries) the oxygen intensity drops to zero very rapidly, it drops only to about 20 % of the maximum intensity in the depth profiles of samples with open grain boundaries (Fig. 5, sample No. 5). This is a direct consequence of the presence of open grain boundaries, since during contact with air not only the "visible" surface of the metallic overlayer but also the "inner" surfaces of the open grain boundaries can be oxidized. This leads to the presence of oxygen within the overlayer which then contributes to the oxygen profile in deeper layers.

It should be noted that the oxygen intensity in such profiles drops to zero before the interface between Ti and the copper substrate is reached. This indicates that a small fraction of the Ti-layer close to the interface is free from open grain boundaries; the Ti-crystallites must have grown together closely in this part of the coating (cf. also SEM photographs in Figs. 1 b and 2 b).

3.2 Effects of Oxidative Treatment

The oxidative attack of the alkaline hydrogen peroxide solution leads to a partial dissolution of the titanium coating. Consequently, one observes a reduction of the overlayer thickness, which has been followed by weight loss, X-ray fluorescence absorption, and AES depth profiles. Changes in the composition of the surface have been followed by XPS. Changes of the in-depth composition have been investigated by AES. The most significant effects have been observed for Ti/Cu samples exhibiting open grain boundaries. The details of the results are described in the following chapters. A summary of various parameters of the investigated samples is given in Tab. 1.

3.2.1 Weight loss and X-ray fluorescence absorption measurements

The reduction of overlayer thickness with etch time was investigated systematically for samples with a 3 μm coating of titanium. The measurements yielded a linear relation between etch time and thickness reduction for samples with open grain boundaries as well as for samples without open grain boundaries. Fig. 11 shows the results for both types of samples. The slopes of the curves are $0.108 \mu\text{m} \cdot \text{min}^{-1}$ for samples with open grain boundaries (thickness reduction determined by X-ray fluorescence absorption and by weight loss measurements) and $0.045 \mu\text{m} \cdot \text{min}^{-1}$ for samples without open grain boundaries (thickness reduction determined by X-ray fluorescence absorption), respectively. The smaller etch rates for samples without open grain boundaries is possibly due to the much smaller surface accessible to the oxidizing solution in contrast to samples with open grain boundaries.

3.2.2 Roughness and topography change measurements

After etching the surfaces of both sample types with and without open grain boundaries they become more structured both looking grit-like (Fig. 12 a, 13 a). While the open grain boundaries seem to be attacked throughout the whole thickness of the layer so that more and larger spaces between the grains become visible (Fig. 12 b), the layers without open grain boundaries seem to remain undisturbed below the thin oxidic layer (Fig. 13 b). This could also be seen after removing the oxide layer by sputtering because the mirror-like surface appeared again.

The values R_a and R_T determining the roughness of the surface showed only a small increase with increasing oxidation time. For a sample without open grain boundaries oxidized for ten minutes the roughness parameters were $R_a = 10 \text{ nm}$ (in comparison to 7 nm for untreated samples) and $R_T = 60 \text{ nm}$ (in comparison to 45 nm), respectively. For a sample with open grain boundaries oxidized for one minute the values were $R_a = 18 \text{ nm}$ and $R_T = 135 \text{ nm}$ (in comparison to 14 and 114 nm for untreated samples), respectively. These small changes are partly due to the effect that the dimensions of the structures are too small to be measured correctly with the stylus of the step-profiler used. Therefore, these measurements revealed only restricted information on the change of the surface topography with increasing oxidation time.

3.2.3 Results of XPS and AES measurements

a) Samples with open grain boundaries in the Ti-coating

Fig. 14 shows an XPS overview spectrum of sample No. 6, which has been oxidized for about 3 min. Besides C, Ti and O, signals from Na and Cu were observed. It is suggested that Na has been adsorbed from the alkaline solution. In case of Cu the signals either result from the excitation of Cu-photoelectrons from the cut faces of the sample plates or from Cu dissolved from the rear side of the plate and redeposited on the coated face. The XPS spectra of Ti 2p and O 1s are shown in Fig. 15. The only difference to the not-oxidized sample No. 1 (cf. Fig. 4) is the absence of the metal peak. This indicates a thicker dioxide overlayer absorbing the Ti 2p metal photoelectrons completely. This assumption is confirmed by the AES depth profiles (see below). As far as XPS spectra have been measured for other samples oxidized for different time intervals they show no significant variations when compared to Figs. 14 and 15.

The AES depth profiles of oxidized samples with open grain boundaries show, in contrast, drastic effects with increasing etch times. After short oxidation time (1 min) the profile is still comparable to that of the untreated sample (cf. Fig. 5) except of the shorter sputtering time necessary to reach the interface, which indicates a partial dissolution of the Ti-coating. Longer oxidation times lead to an increasing oxygen concentration within the overlayer. This is demonstrated in Fig. 16 for sample No. 3 with an oxidation time of about 5 min. Corresponding selected AES spectra are shown in Fig. 17. After an extended region of constant composition with high oxygen content the O 1s signal intensity drops rapidly when approaching the Ti/Cu-interface while the Ti-intensities first increase before the expected decrease at the real interface. This behaviour is similar to that of the untreated samples with open grain boundaries (cf. Fig. 5) indicating a significant influence of the latter on the oxidation process. This will be discussed in context with the chemical speciation results below.

Extended etching (≥ 10 min) of samples with 1 μm thick Ti-coating with open grain boundaries results in depth profiles which indicate a destruction of the overlayer. An example is shown in Fig. 18, corresponding selected AES spectra in Fig. 19. The presence of Cu after very short sputtering times indicates breaks in the Ti-coating. The shapes of the O- and Ti-profiles, which have pronounced maxima, point to an island-like structure of the remaining parts of the overlayer. The different positions of the O- and Ti-maxima indicate that the inner parts of the islands are still metallic. The gradual increase of the copper intensities supports the proposed island structure and, in addition, shows that the islands have significantly differing thicknesses.

A quantitative evaluation of the almost equal intensities of Ti and O in samples with open grain boundaries after medium etch times, which was based on a comparison of the relative O(KLL) and Ti(L₃M₂₃M₂₃)-intensities in several titanium oxides, yielded an integral composition of the major part of the overlayer corresponding approximately to the stoichiometry of TiO (30). It was, however, pointed out in this reference that this result cannot be interpreted exclusively by the presence of titanium monoxide since not only a homogeneous TiO-layer but also an inhomogeneous mixture of TiO₂ and Ti-metal both lead to equally shaped AES spectra. A distinction between these two possibilities can be made by XPS investigations. Fig. 20 shows a sequence of Ti 2p XPS-spectra of sample No. 6 taken at different depths of the overlayer. The uppermost spectrum (already shown in Fig. 15) represents TiO₂. With increasing depth a second Ti-component at about 454 eV appears. The lower two spectra were both recorded in the plateau region of the depth profile (cf. Fig. 16, profile type "B"). In these spectra the Ti 2p_{3/2} binding energy (454.3 eV) is very close to that of pure Ti-metal (454.0 eV, Ref. 27), but a direct comparison with the spectrum of Ti-metal, which is given in Fig. 21 b, shows distinct differences as can be seen from the hatched area in Fig. 21 a. After subtraction of the Ti-metal component from the spectrum of sample No. 6 (Fig. 20 c) there remains a residual multiplet (Fig. 22 a), which can be resolved into three components as shown in Fig. 22 b. According to published binding energy values (27) these components can be assigned to TiO, Ti₂O₃, and TiO₂.

To explain the origin of these suboxides one has to keep in mind that after sputtering the Ti 2p spectra (Fig. 20 c and similarly 20 d) represent not only the original composition of the overlayer at the corresponding depth but also the influence of ion bombardment which is known to reduce Ti⁴⁺ to Ti³⁺ and Ti²⁺ (but not to the metal cf. Refs. 27, 28). Therefore it is very likely that the observed spectra result from a mixture of Ti-metal and TiO₂, the latter compound being partially reduced by ion bombardment. Furthermore, the existence of a homogeneously oxidized TiO-overlayer, which was the other possibility of explaining the observed Auger spectra, is clearly ruled out because in this case the XPS spectra should show one single component (TiO) at a binding energy of 455.5 eV (Ti 2p_{3/2}) which is definitely different from the observed value of 454.3 eV.

With respect to the alkaline hydrogen peroxide treatment this result indicates that the oxidative attack besides a partial dissolution of the metallic overlayer, leads to the formation of TiO₂, which is not dissolved. The open grain boundaries permit an oxidation not only at the "visible" surface but also "within" the overlayer leading to the "coexistence" of Ti-metal and TiO₂ in the plateau region of the profile (cf.

Fig. 16). While the metal component represents the inner part of the individual grains not yet oxidized, the dioxide reflects the oxidation at the grain boundaries. This picture also explains the rapid drop of the oxygen concentration close to the interface and the corresponding increase of the metal intensity: here the grains have grown closely together without exhibiting attackable open boundaries.

These explanations are also valid for the unetched Ti/Cu-substrates with the open grain boundaries oxidized by atmospheric contact only.

These explanations of the observed spectra and profiles are supported by published results showing on one hand that an oxidative treatment of Ti and Ti-based alloys leads to the formation of TiO_2 (5) and on the other hand that, depending on the etching conditions, grain boundaries may be attacked preferentially (8). Other authors, however, observe the formation of an amorphous, non-stoichiometric oxidic phase (17).

b) Samples without open grain boundaries in the Ti-coating

The depth profiles of oxidized samples no. 10 to 15 are, in principle, comparable to that of the corresponding unoxidized sample (no. 9, cf. Fig. 8). Differences are observed with respect to the total overlayer thickness, which is continuously reduced with increasing etch time (cf. Fig. 11). In addition, the thickness of the dioxide overlayer increases with etch time as illustrated in Fig. 23. The unoxidized sample has an oxide layer thickness of about 3 nm which increases to about 40 nm after 20 min etching.

The dissolution of the titanium overlayer seems to take place in a very regular manner. This statement is based on a comparison of the absolute widths of the Ti/Cu-interfaces in the profiles of samples no. 9 and 13. The interface width of sample no. 13 is only insignificantly larger than that of sample no. 9. In case of a very irregular attack (e.g. preferentially at grain boundaries) one would expect an additional distortion of the profile at the interface between Ti-coating and Cu-substrate due to an irregular thickness of the coating.

3.2.4 Results on bonding properties

In Fig. 24 the percentage of structures with a diameter of 5 μm is shown which do not adhere to the etched Ti-surface as a function of etch time. In this case the Ti-surface was produced without open grain boundaries. For etch times less than 5 min

this percentage increases strongly. For an etch time of 3 min, for example, not only 50 % of the structures with 5 μm diameter but even part of the 10 μm structures did not adhere to the substrate. For etch times less than 1 min the polymerized PMMA-layer as a whole did not stick to the Ti-surface. For etch times larger than 6 min no significant adhesion problems are encountered as long as the etch time is shorter than the time needed to remove nearly all the Ti-coating which is indicated by large uncovered parts of the Cu-surface. This limit is reached, e.g. for 1 μm thick Ti-coatings produced with open grain boundaries by sputtering after etch times beyond 10 min (cf. Fig. 24, samples No. 4 and 8, and Table 1). Consequently, for optimum adhesion properties etch times must be between 6 min and the upper limit defined by the removal time for the Ti-coating. This latter time depends on the layer thickness as well as on the structure of the overlayer.

3.3 Correlation of Surface Analyses and Bonding Properties

The basic question giving rise to the present investigation was for the mechanism responsible for the bonding between the Ti-coating and the PMMA. The results on bonding properties revealed that - more or less independent on the structure of the Ti-coating - an etching treatment for a minimum time interval is necessary in order to obtain satisfactory bonding. At present, we see three principal mechanisms which could cause the bonding:

- (i) formation of chemical bonds between the oxidized Ti-surface and the PMMA,
- (ii) "rough structures" with sizes in the μm -range like e.g the observed open grain boundaries, eventually after enlarging by oxidative attack,
- (iii) "microstructures" with sizes in the nm-range like micropores as observed by several authors (Refs. 31-36).

From the combined bonding property- and surface analytical investigations the first two possibilities mentioned above can be clearly ruled out:

- (i) For any chemical bonding only the outermost atomic layers of polymer and substrate are responsible. However, the AES depth profiles showed that a TiO_2 layer of 20 - 40 nm thickness is necessary to obtain good bonding properties. In contrast, a chemical bonding should be possible even with an oxide layer of only a few nm thickness already present on the untreated samples or after very short etch times.

- (ii) There was no influence observed of open grain boundaries on the bonding properties of different Ti-coatings. Both sample types with and without open grain boundaries showed similar bonding behaviour after the generation of an approximately 30 nm thick TiO₂ layer (cf. Table 1).
- (iii) The micropores, which according to Refs. (31,32,34,36) in fact exist in oxidic overlayers, become effective for bonding possibly only after the oxidic layer has grown to a minimum thickness and, consequently, after the pores have attained a definite size (diameter and depth). In this case the bonding would be an effect of mechanical interlocking of the polymerized molecules with micropores of proper size.

Though we cannot prove this latter mechanism directly, it seems to be the most likely one, since it is in accordance with all observations presented in the foregoing chapters.

4. Summary

The optimization of bonding between Ti-coated Cu-substrates and PMMA-microstructures by means of an oxidative pretreatment of the Ti-surface with alkaline peroxide solution was originally a more or less heuristic procedure in course of the LIGA process. In addition, the influence of different structures of the coating originating from different conditions during sputter-deposition of Ti was not well understood since the mechanism responsible for the bonding effect was unknown. Surface analytical investigations by XPS-measurements, AES- and XPS-depth profiles showed a continuous and regular build-up of a homogeneous oxide layer consisting mainly of TiO₂. In addition, it could be demonstrated that the oxidative attack in case of Ti-coatings with open grain boundaries proceeds to a significant extent along these grain boundaries. This leads finally to breaks in the coating and to uncovered parts of the Cu-substrate with islands of Ti-metal in between. In contrast, for samples without open grain boundaries a rather regular removal of the metallic layer accompanies the build-up of the oxidic overlayer.

The comparison of the investigated bonding properties in dependence on the etch times to the respective surface structures showed that, regardless of the presence of open grain boundaries, an oxide layer thickness of at least 30 nm is necessary to obtain good bonding. On the other hand, this bonding is only continuing as long as the oxidic layer remains closed. A partial removal of the whole coating (Ti-oxide and -metal) reduces bonding drastically since PMMA does not adhere at all to a Cu-

surface. From these findings we concluded that bonding between Ti-coating and PMMA-structures is neither caused by chemical effects, which should already act with a few oxide monolayers, nor by the influence of the open grain boundaries, but rather by a kind of micropores, which become of proper size only in oxide layers of more than 30 nm thickness. A direct proof of this mechanism was not possible in the framework of the present experiments. It could be done, however, by producing a pore-free closed TiO₂-layer, e.g. by means of reactive sputtering of Ti in an oxygen atmosphere. In this case, one would expect poor or no bonding even for oxide layers of proper thicknesses.

With respect to the LIGA-process the results obtained in the present investigation show that it is preferable to use samples with Ti-layers without open grain boundaries, since the etch rate is significantly smaller. The oxidic overlayer becomes sufficiently thick for optimum bonding after oxidation times larger than 6 min. It seems to be sufficient to use Ti-layers of ca. 0.4 µm thickness as adhesion layers. When etching Ti mask membranes one must keep in mind that etching causes a decrease in thickness. On the other hand, the necessary oxidic overlayer is very thin and should, therefore, not influence the mechanical stability of the membrane.

Acknowledgement

The help of Dr. G. Linker, Institut für Nukleare Festkörperforschung, KfK Karlsruhe, who performed the Rutherford Backscattering measurement, is gratefully acknowledged.

References

1. I. Ruge in "Halbleitertechnologie", 2. ed. Chapt. 8, Springer-Verlag, Berlin (1984).
2. W. Ehrfeld, W. Glashauser, D. Münchmeyer, and W. Schelb, *Microelectr. Engin.* 5, 463 (1986).
3. E.W. Becker, W. Ehrfeld, P. Hagmann, A. Maner, and D. Münchmeyer, Report KfK-3995 (1985).
4. E.W. Becker, W. Ehrfeld, and D. Münchmeyer, Report KfK-3732 (1984).
5. M. Assepour-Dezfuly, C. Vlachos, and E.H. Andrews, *J. Mat. Sci.* 19, 3626 (1984).
6. J.D. Venables, D.K. McNamara, J.M. Chen, T.S. Sun, and R.L. Hopping, *Appl. Surf. Sci.* 3, 88 (1979).
7. G.D. Davis, T.S. Sun, J.S. Ahearn, and J.D. Venables, *J. Mat. Sci.* 17, 1807 (1982).
8. K.W. Allen, H.S. Alsalim, and W.C. Wake, *J. Adh.* 6, 153 (1974).
9. D.M. Brewis (Ed.), "Surface Analysis and Pretreatment of Plastics and Metals", Chapt. 7 and 8, Applied Science, Barking (1982).
10. L.A. Casper and C.J. Powell (Eds.), "Industrial Applications of Surface Analysis", Chapt. 7, ACS Symp. Ser. 199, Washington DC (1982).
11. R. Houwink and G. Salomon (Eds.), "Adhesion and Adhesives", Vol. 2, Chapt. 12, Elsevier Publ. Comp., Amsterdam (1965).
12. R. Houwink and G. Salomon (Eds.), "Adhesion and Adhesives", Vol. 1, Chapt. 1, Elsevier Publ. Comp., Amsterdam (1965).
13. E.H. Andrews, He Pingsheng, and C. Vlachos, *Proc. Roy. Soc. Lond.* A381, 345 (1982).
14. I. Lhermitte-Sebire, R. Colmet, R. Naslain, J. Desmaison, and G. Gladel, *Thin Solid Films* 138, 221 (1986).
15. I. Lhermitte-Sebire, H. Lahaye, R. Colmet, R. Naslain, and M. Chevrier, *Thin Solid Films* 138, 209 (1986).
16. A. Pan and J.E. Greene, *Thin Solid Films* 97, 79 (1982).
17. A. Mahoon and J. Cotter, Proc. 10th Nat. SAMPE Technical Conf., Kiamesha Lake, NY, 1978, p. 425, SAMPE, Azusa CA (1978).
18. W.L. Baun, *Appl. Surf. Sci.* 4, 291 (1980).
19. W.J. van Ooij, A. Kleinhesselink, and S.R. Leyenaar, *Surf. Sci.* 89, 165 (1979).
20. W.J. van Ooij and A. Kleinhesselink, *Appl. Surf. Sci.* 4, 324 (1980).
21. J.A. Thornton, *Ann. Rev. Mater. Sci.* 7, 239 (1977).
22. B.A. Movchan and A.V. Demchishin, *Phys. Met. Metallogr.* 28, 83 (1969).
23. J.A. Thornton, *J. Vac. Sci. Techn.* 11, 666 (1974).

24. H.-H. Behncke, "Einführung in die Schichtdickenmessung nach dem Röntgenfluoreszenzverfahren", Firmenschrift Fa. Fischer GmbH, Sindelfingen.
25. H. Moers, PhD Thesis, University of Karlsruhe (1986), Report KfK-4073 (1986).
26. J.A. Marceau, Y. Moji, and J.C. Mcmillan, *Adhesive Age* 20, No. 10, 332 (1977).
27. G. Pfennig, H. Moers, H. Klewe-Nebenius, R. Kaufmann, and H.J. Ache, *Microchim. Acta*, Suppl. 11, 113 (1985).
28. S. Hofmann and J.M. Sanz, *J. Trace Microprobe Techn.* 1, 213 (1982-1983).
29. R. Kaufmann, Master Thesis, University of Karlsruhe (1985).
30. H. Moers, H. Klewe-Nebenius, and G. Pfennig, Report KfK-4221 (1987).
31. D.E. Packam in: *Adhesion Aspects of Polymeric Coatings*, K.L. Mittal (ed.), Plenum Press N.Y. (1983).
32. O.-D. Hennemann and W. Brockmann, *J. Adhesion* 12, 297 (1981).
33. J.D. Venables, D.K. McNamara, J.M. Chen, B.M. Ditchek, T.I. Morgenthaler, T.S. Sun, and R.L. Hopping, Proc. 12th Nat. SAMPE Technical Conf., Seattle, WA, 1980, p. 909, SAMPE, Azusa, CA (1980).
34. B.M. Ditchek, K.R. Breen, T.S. Sun, and J.D. Venables, Proc. 25th SAMPE Symposium and Exhibition, p. 13 (1980).
35. B.M. Ditchek, K.R. Breen, T.S. Sun, and J.D. Venables, Proc. 12th Nat. SAMPE Technical Conf., Seattle, WA, 1980, p. 882, SAMPE, Azusa, CA (1980).
36. J.D. Venables, *J. Mat. Sci.* 19, 2431 (1984).

Table 1 Summary of etch times, coating and overlayer thicknesses, and bonding properties of the investigated Ti/Cu-samples

Sample No. a)	Etch Time (min)	Coating Thickness nominal ^{b)} (nm)	Coating Thickness AES ^{c)} (nm)	Relative Coating Thickness			Depth Profile Type ^{k)}	TiO ₂ -Over-layer Thickness (nm)	Bonding Properties
				AES	Wt. loss ^{l)}	X-Ray Abs.			
1	0	1000	850	1	1	1	A	3	bad
2	1	1000	720	0.85 ^{d)}	0.64	0.69	A	~ 7	bad
3	5	1000	610	0.72 ^{d)}	0.4	0.28	B	38	satisfact.
4	15	1000	~250	~ 0.29 ^{d)}	0.26	0.21	C	-	bad
5	0	1000 ^{e)}	885±5 ^{f)}	1	1	1	A	3	bad
6	3	1000	670	0.76 ^{g)}	0.63 ^{g)}	0.67 ^{g)}	B	22	good
7	0	1000	890	1	1	1	A	3	bad
8	10	1000	210	~ 0.24 ^{h)}	0.33 ^{h)}	0.19 ^{h)}	C	-	bad
9	0	3000	2860	1	1	~ 1	D	3	bad
10	1	3000	-	-	-	~ 1 ⁱ⁾	-	14	bad
11	13	3000	-	-	-	0.92-0.95 ⁱ⁾	-	32	satisfact.
12	5	3000	-	-	-	0.90	-	24	good
13	10	3000	2230	0.78 ⁱ⁾	-	0.85	D	33	very good
14	15	3000	-	-	-	0.79	-	38	very good
15	20	3000	-	-	-	0.73	-	42	good

Footnotes Table I

- a) Samples no. 1-8: with open grain boundaries
no. 9-15: without open grain boundaries
- b) Approximate thickness of Ti-coating before oxidative treatment (values strived for by sputter deposition of Ti).
- c) Calculated from the experimental current density and the sputtering rate of Ti-metal ($2.14 \text{ nm} \cdot \text{min}^{-1}$ at $200 \text{ nA} \cdot \text{mm}^{-2}$ (29)).
- d) Samples no. 1-4 represent a series produced under identical conditions before etching. Sample no. 1 was used as standard for samples no. 2-4.
- e) For this sample the thickness of the Ti-overlayer has been determined independently by means of Rutherford Backscattering Spectroscopy (RBS) to be $885 \pm 5 \text{ nm}$ under the assumption of a pure Ti-metal overlayer. This method is described in detail in Ref. (29).
- f) The RBS thickness of this sample (cf. footnote e)) was used to calibrate the ion current density measurements for the depth profiles of samples no. 6-15.
- g) Coating thickness relative to that of sample no. 5.
- h) Coating thickness relative to that of sample no. 7.
- i) Coating thickness relative to that of sample no. 9.
- k) The classification of the different depth profiles has been introduced in order to mark similarity of the observed depth distributions. A typical profile of type A is shown in Fig. 5, examples of types B, C, and D are displayed in Figs. 16, 18, and 8, respectively.

Figure Captions

- Fig. 1: SEM-photograph of an untreated Ti-surface without open grain boundaries
a) surface b) cross section
- Fig. 2: SEM-photograph of an untreated Ti-surface with open grain boundaries
a) surface b) cross section
- Fig. 3: XPS overview spectrum (excitation: Al K α -radiation) of sample no. 1, representing the surface composition of an untreated Ti-overlayer with open grain boundaries. The main photopeaks of Ti, O and C have been marked. The peaks at high binding energies result from Auger transitions in Ti and O.
- Fig. 4: XPS element spectra (Al K α -excitation) of sample no. 1 at the Ti 2p and O 1s energies.
- Fig. 5: AES depth profile of sample no. 5 (with open grain boundaries, Ti-coating thickness: 1 μ m, untreated). Profiles of this shape are termed to be of "type A".
- Fig. 6: Depth profile of the surface-near part of the Ti-coating of sample no. 5.
- Fig. 7: Auger spectra corresponding to specific sputtering times of the profile of Fig. 5. The assignment of the main Auger peaks is as follows: Cu (L₃VV) = 920 eV, O (KLL) = 515 eV, Ti(L₃M₂₃V) = 420 eV, Ti(L₂M₂₃M₂₃) = 385 eV.
- Fig. 8: AES depth profile of sample no. 9 (without open grain boundaries, Ti-coating thickness: 3 μ m, untreated). Profiles of this shape are termed to be of "type D".
- Fig. 9: Depth profile of the surface-near part of the Ti-coating of sample no. 9.
- Fig. 10: Auger spectra corresponding to specific sputtering times of the profile of Fig. 8.

- Fig. 11: Ti-layer thickness reduction as a function of etch time for samples with and without open grain boundaries (thickness of Ti-coating: 3 μm).
- Fig. 12: SEM-photograph of a Ti-surface with open grain boundaries after 5 min oxidative treatment
a) surface b) cross section
- Fig. 13: SEM-photograph of a Ti-surface without open grain boundaries after 8 min oxidative treatment
a) surface b) cross section
- Fig. 14: XPS overview spectrum (excitation: Al K_{α} -radiation) of sample no. 6, representing the surface composition of a Ti-overlayer with open grain boundaries after oxidation with alkaline hydrogen peroxide solution. The main photopeaks of the detected elements have been marked. The Auger peaks and minor photopeaks are not assigned.
- Fig. 15: XPS element spectra (Al K_{α} -excitation) of sample no. 6 at the Ti 2p and O 1s energies.
- Fig. 16: AES depth profile of sample no. 3 (with open grain boundaries, Ti-coating thickness: 1 μm , etch time: 5 min). Profiles of this shape are termed to be of "type B".
- Fig. 17: Auger spectra corresponding to specific sputtering times of the profile of Fig. 16.
- Fig. 18: AES depth profile of sample no. 4 (with open grain boundaries, Ti-coating thickness: 1 μm , etch time: 15 min). Profiles of this shape are termed to be of "type C".
- Fig. 19: Auger spectra corresponding to specific sputtering times of the profile of Fig. 18.
- Fig. 20: XPS spectra at the Ti 2p energy of sample no. 6 measured after various sputtering times (Al K_{α} -excitation).

Fig. 21: (a) Ti 2p XPS spectrum of sample no. 6 after sputtering until the composition remained constant. The spectrum is identical to that of Fig. 20 c.

(b) Ti 2p XPS spectrum of pure Ti-metal. The hatched area in the upper spectrum (a) corresponds to the difference of both spectra and indicates the contribution of oxidic Ti-species.

Fig. 22: (a) Difference of the two spectra shown in Fig. 21 a and b (hatched area of Fig. 21 a) after proper normalization.

(b) Result of a multiplet analysis of spectrum (a) after subtraction of background and X-ray satellites. The spectral parameters for the Ti-oxides were taken from Ref. 27.

Fig. 23: Titanium dioxide overlayer thicknesses of Ti/Cu samples without open grain boundaries as a function of etch time. The interface between dioxide and underlying metal is adopted at the point, where the intensities of the Ti(L₃M₂₃M₂₃) and O(KLL) Auger transitions are equal.

Fig. 24: Bonding properties of Ti-coatings as a function of etch time. As a measure for the bonding quality the fraction of microstructures with an adhesion area of $2 \times 10^{-5} \text{ mm}^2$, which do not adhere to the oxidized Ti-surface, is given in dependence on the oxidation time. The data were obtained for samples without open grain boundaries and Ti-overlayer thicknesses of $3 \mu\text{m}$.

1. Data points corresponding to samples no. 1, 9 (not oxidized) and no. 10 (1 min oxidized). In these cases already the whole resist layer did not adhere to the substrate.
2. Data point corresponding to sample no. 4 (with open grain boundaries). In this case the Ti-overlayer was destroyed after etching.

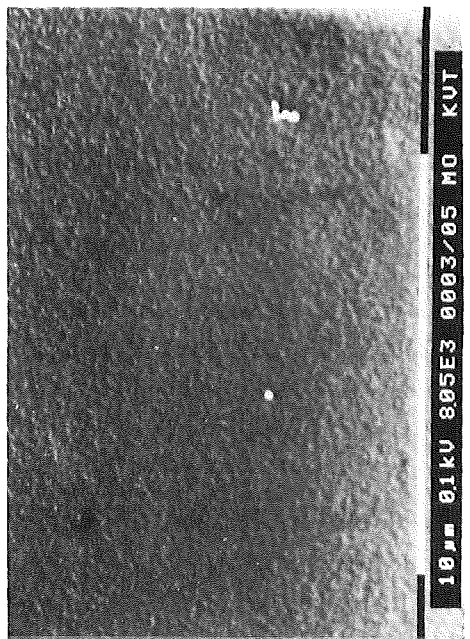


Fig. 1 a

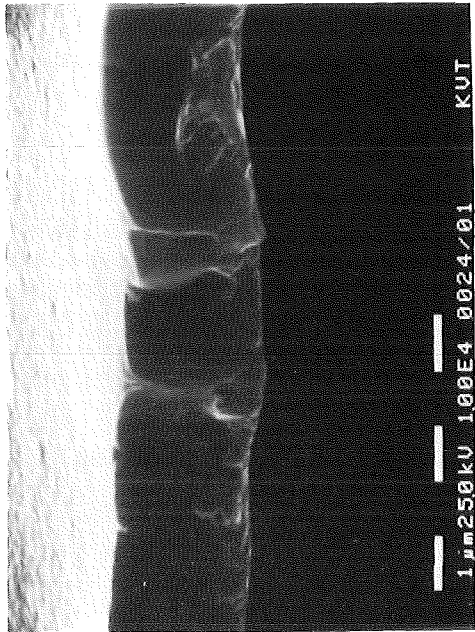


Fig. 1 b

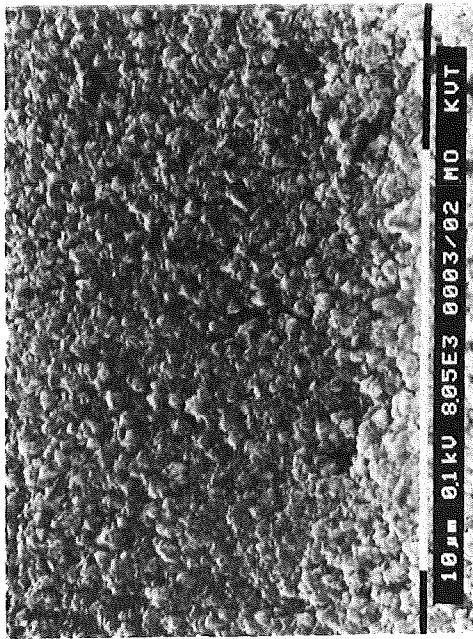


Fig. 2 a

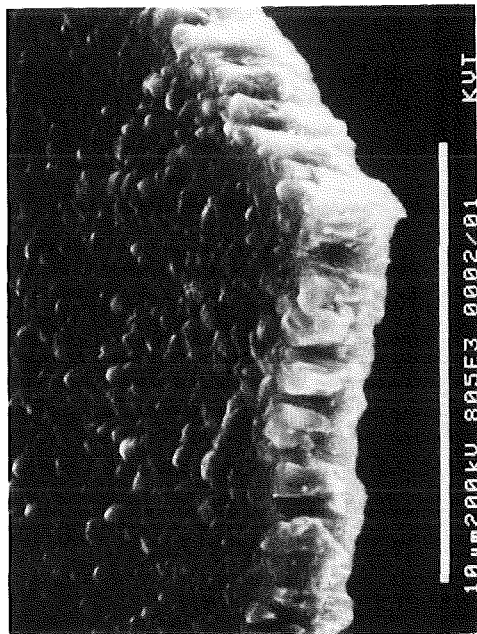


Fig. 2 b

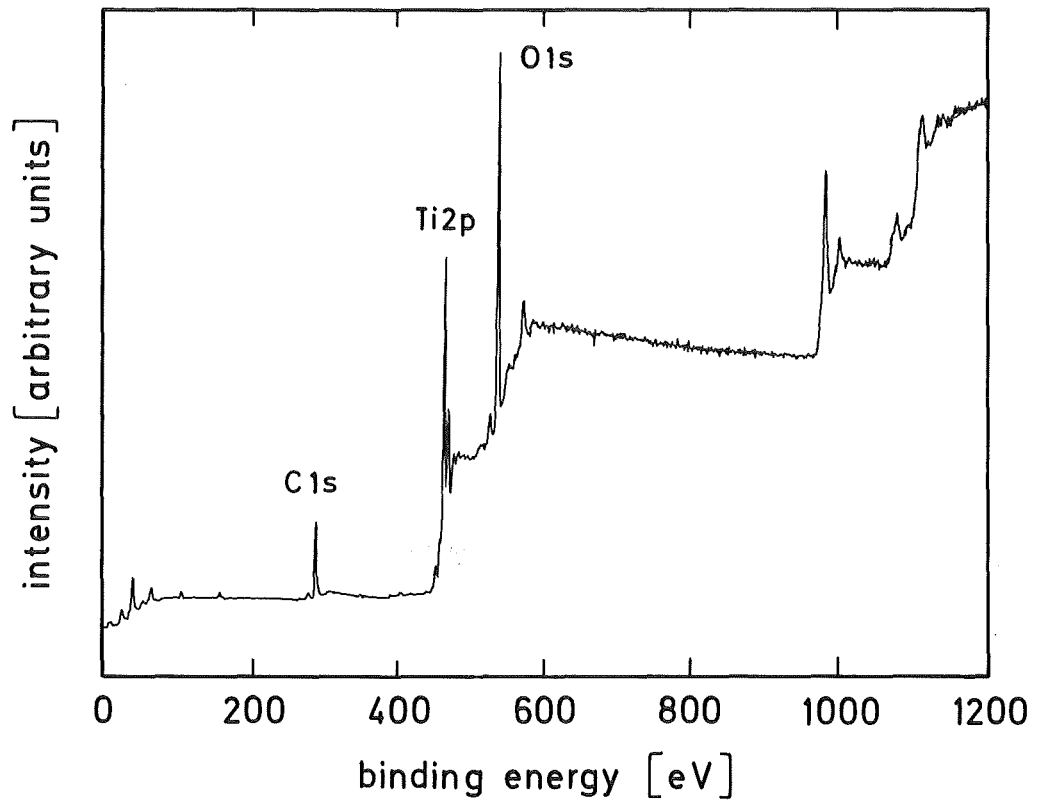


Fig. 3

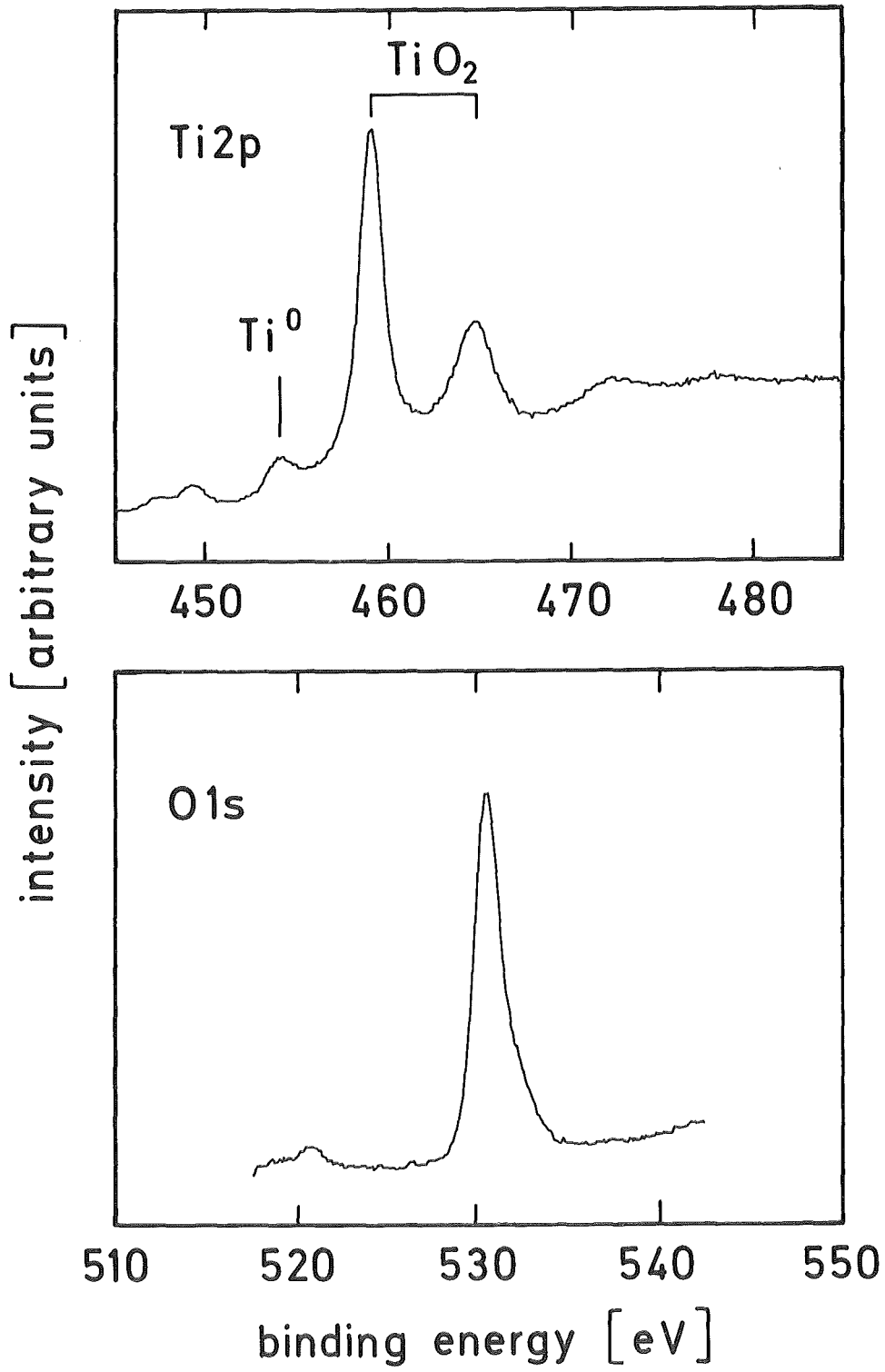


Fig. 4

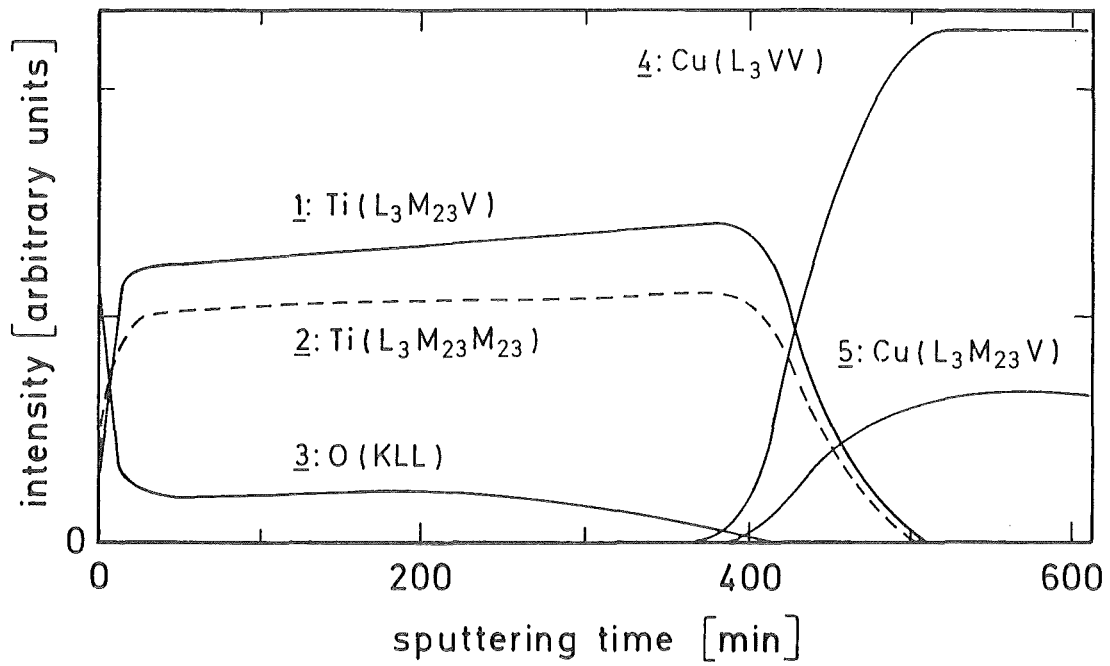


Fig. 5

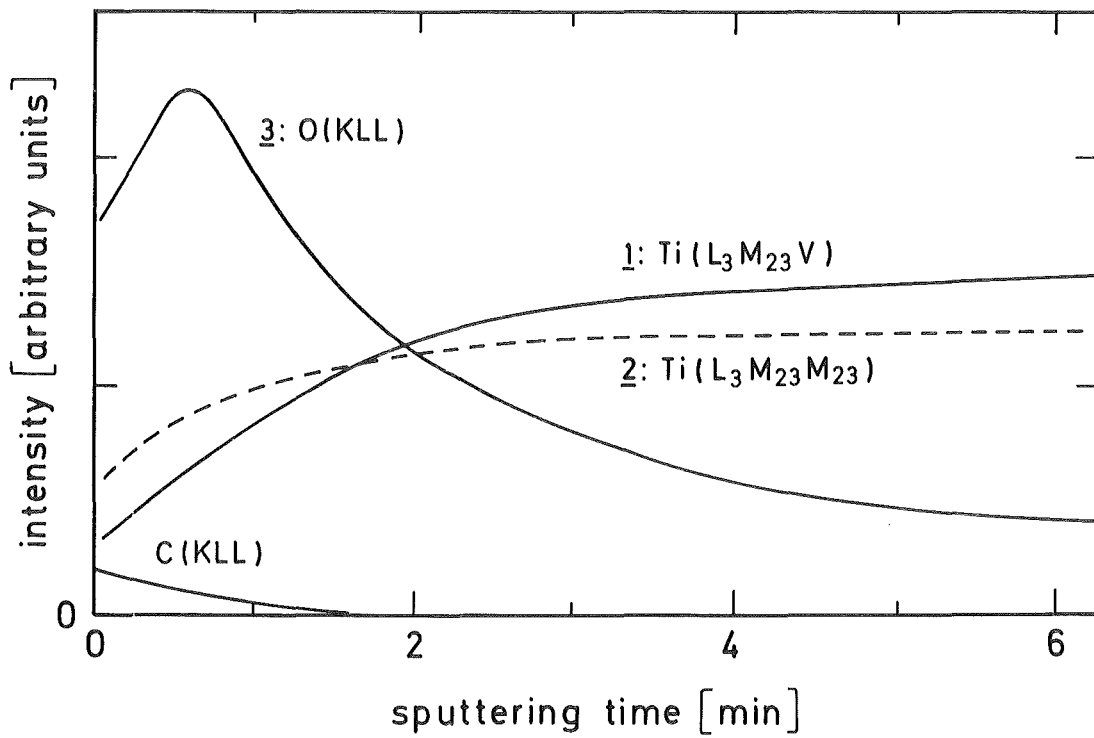


Fig. 6

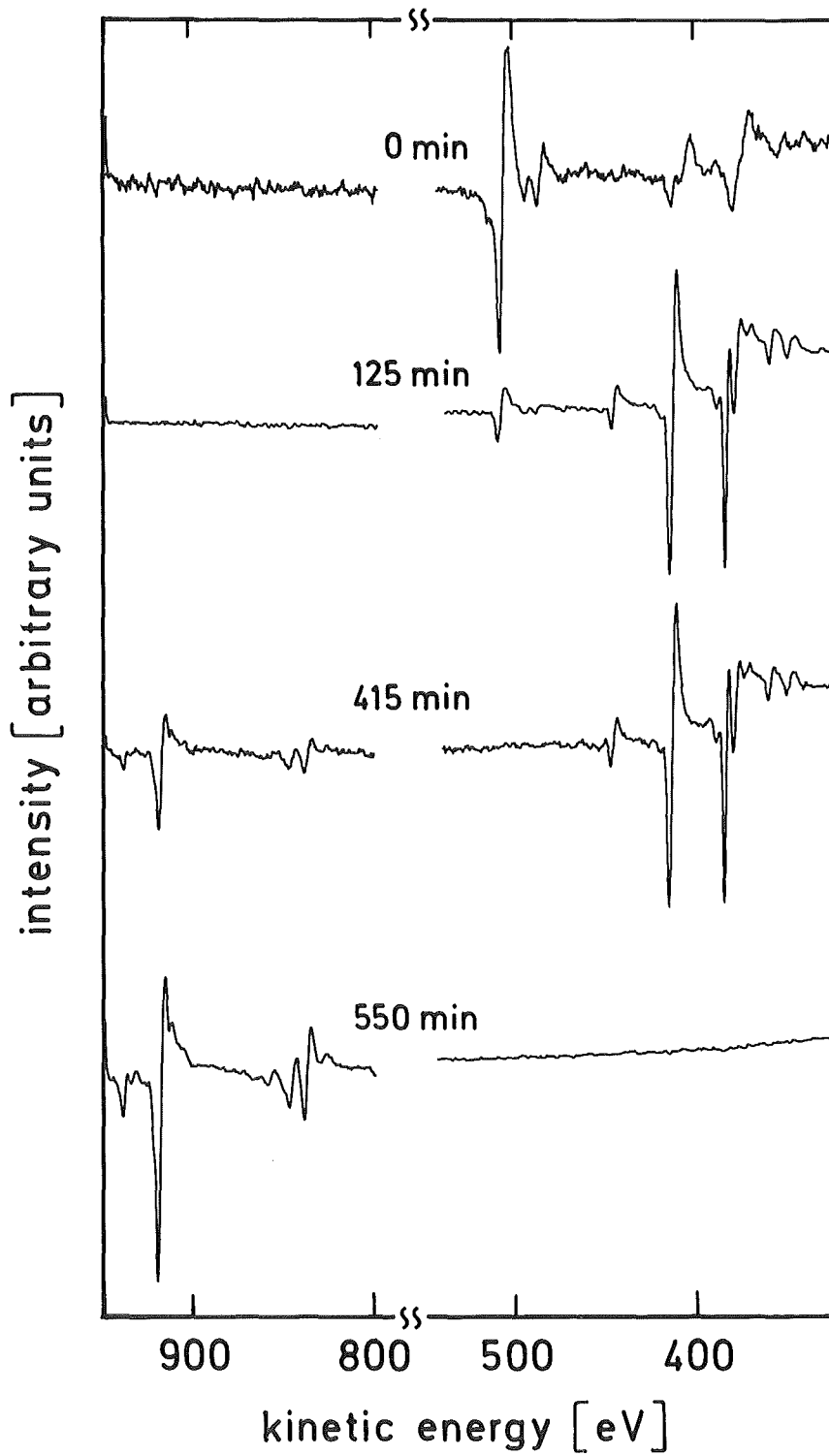


Fig. 7

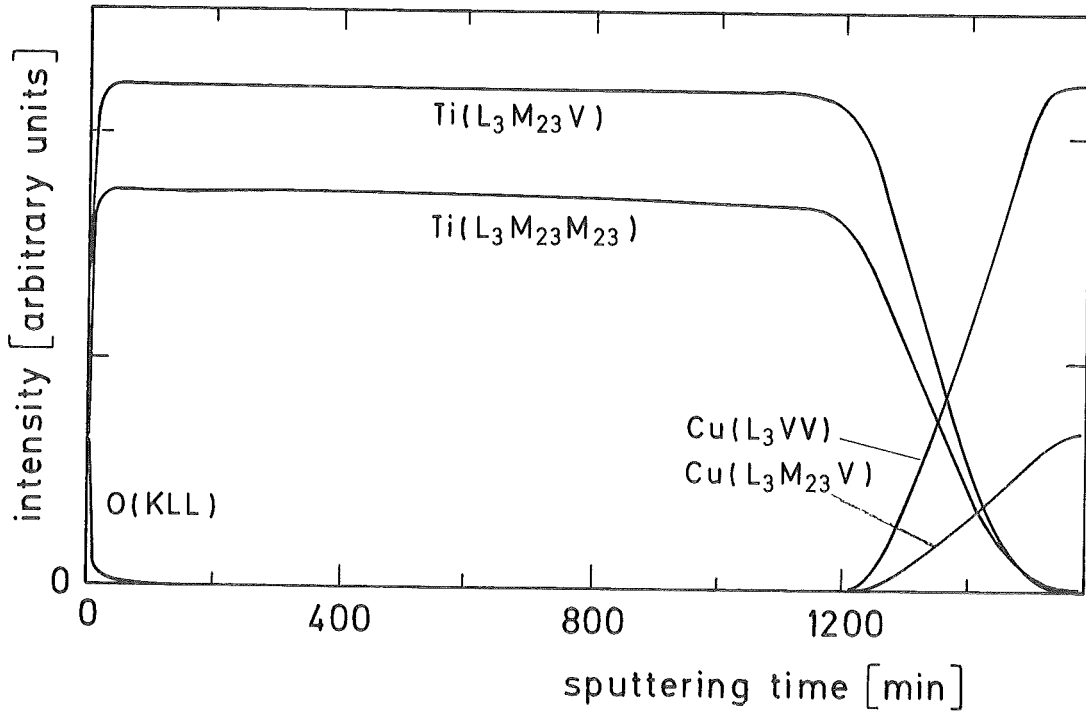


Fig. 8

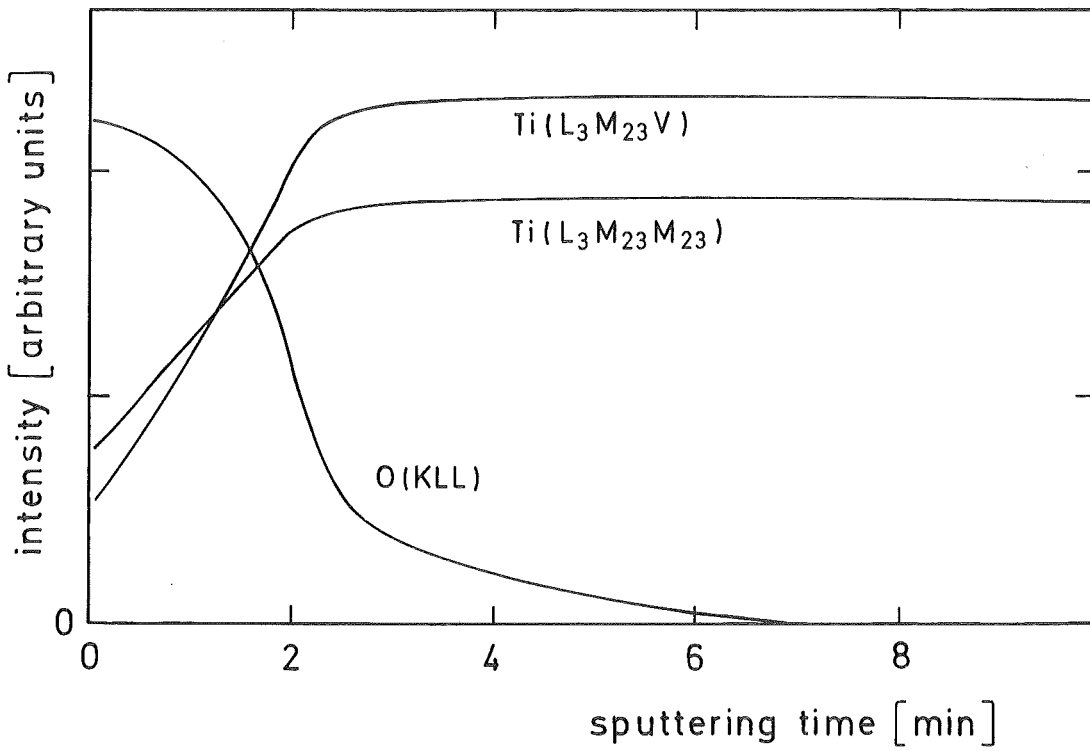


Fig. 9

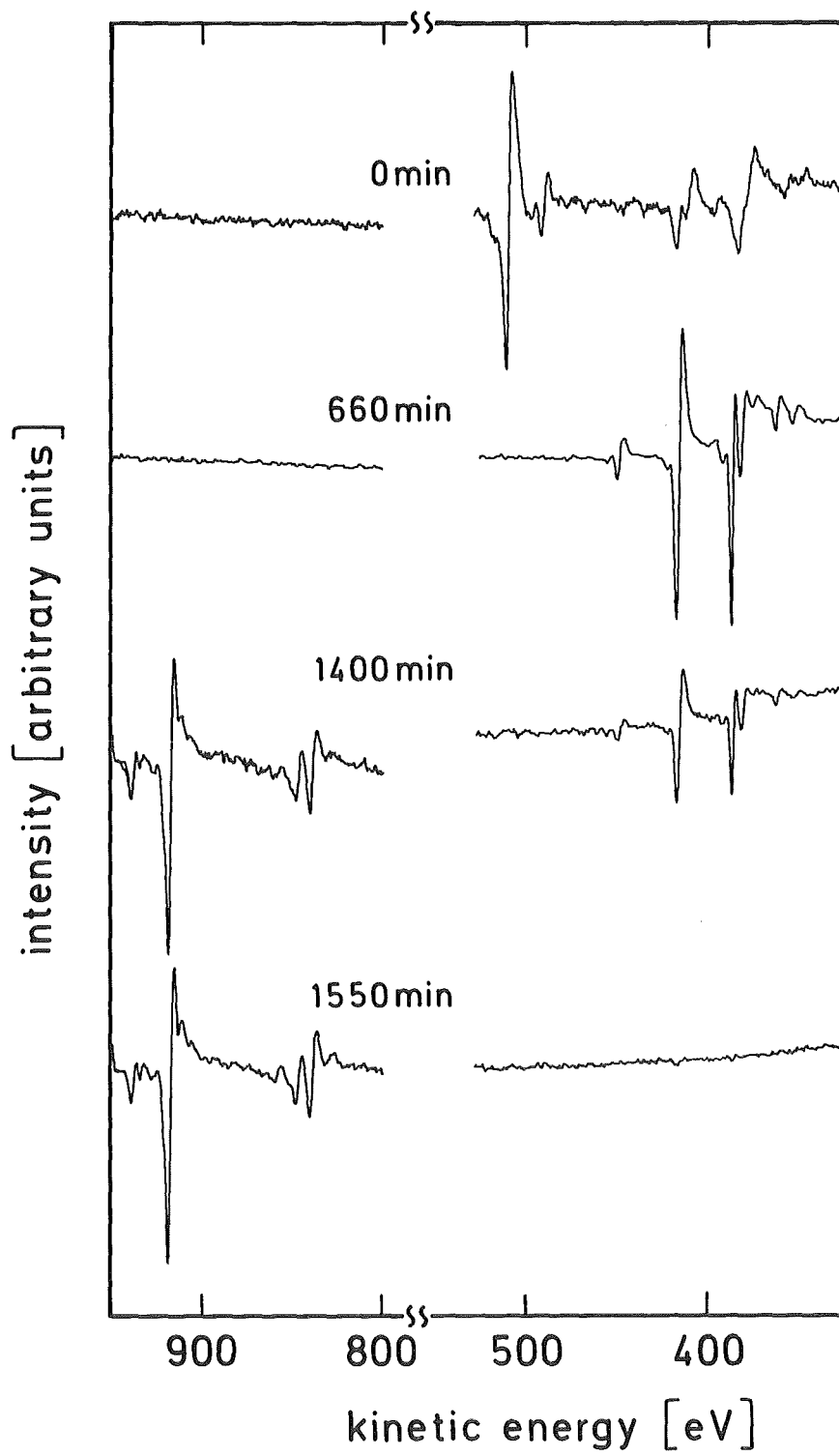
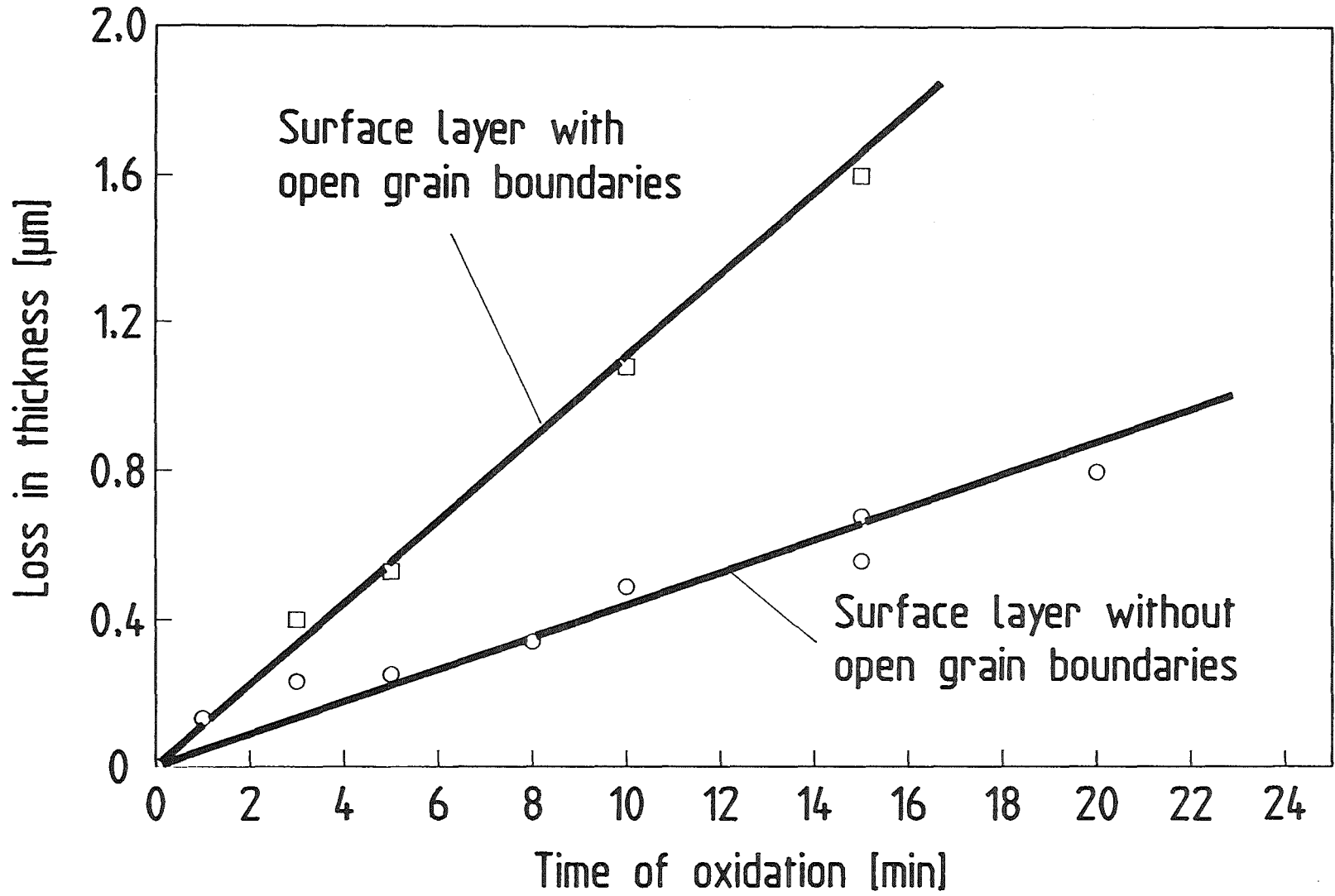


Fig. 10

Fig. 11



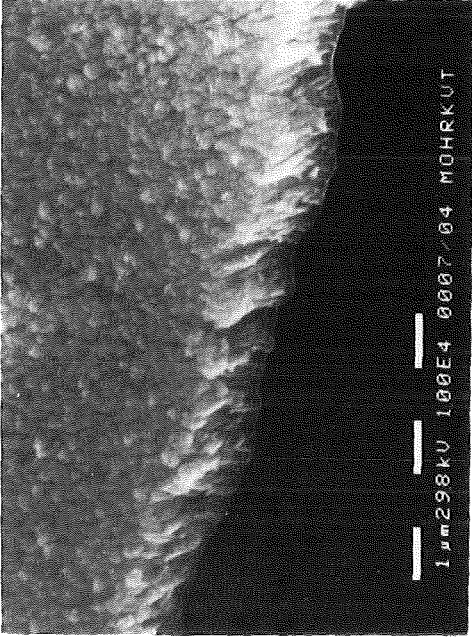


Fig. 12 b

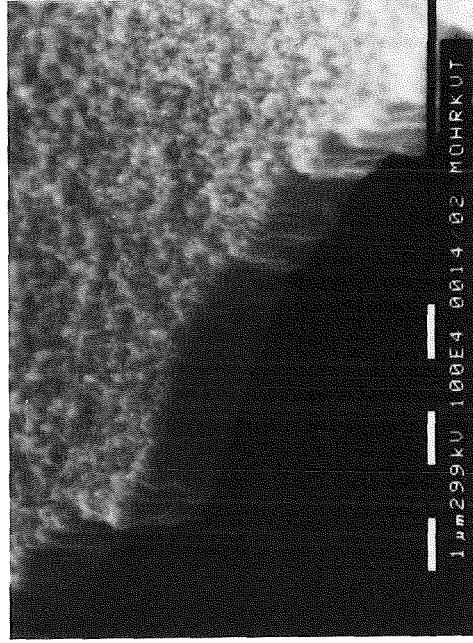


Fig. 13 b

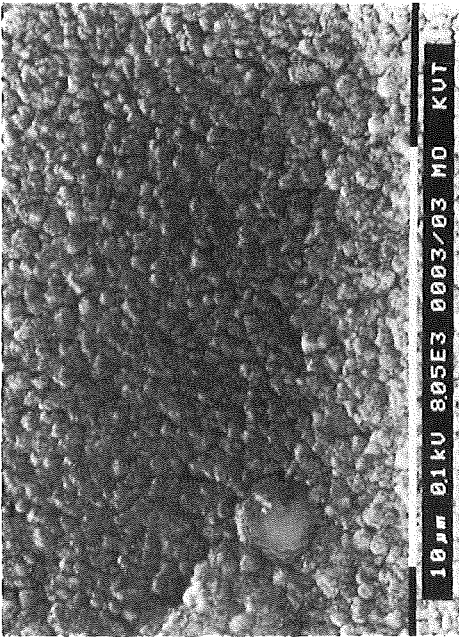


Fig. 12 a

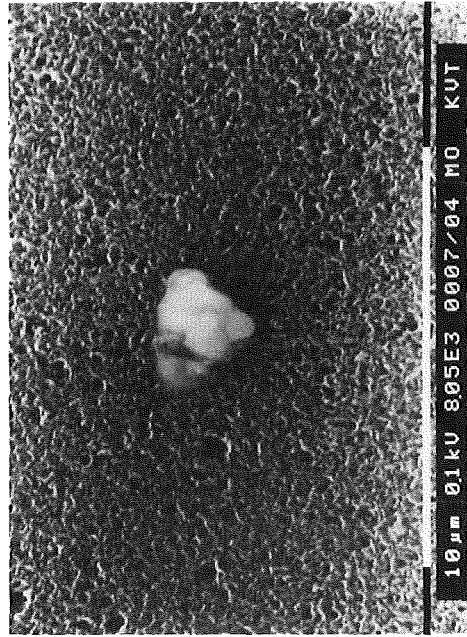


Fig. 13 a

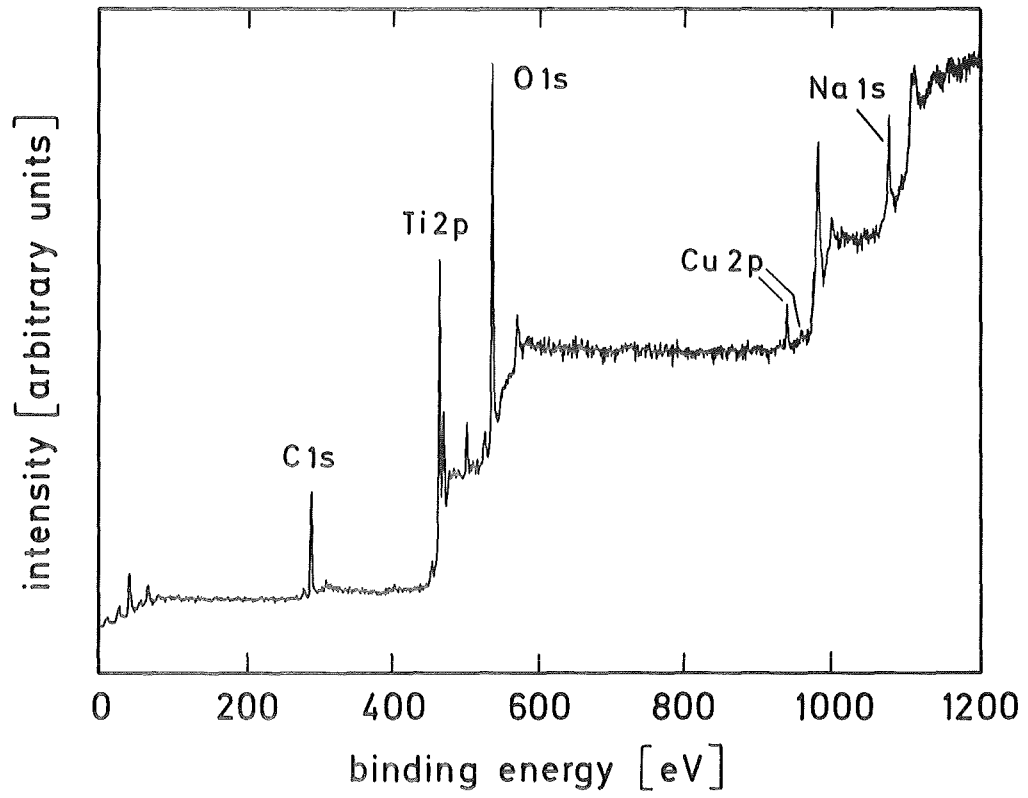


Fig. 14

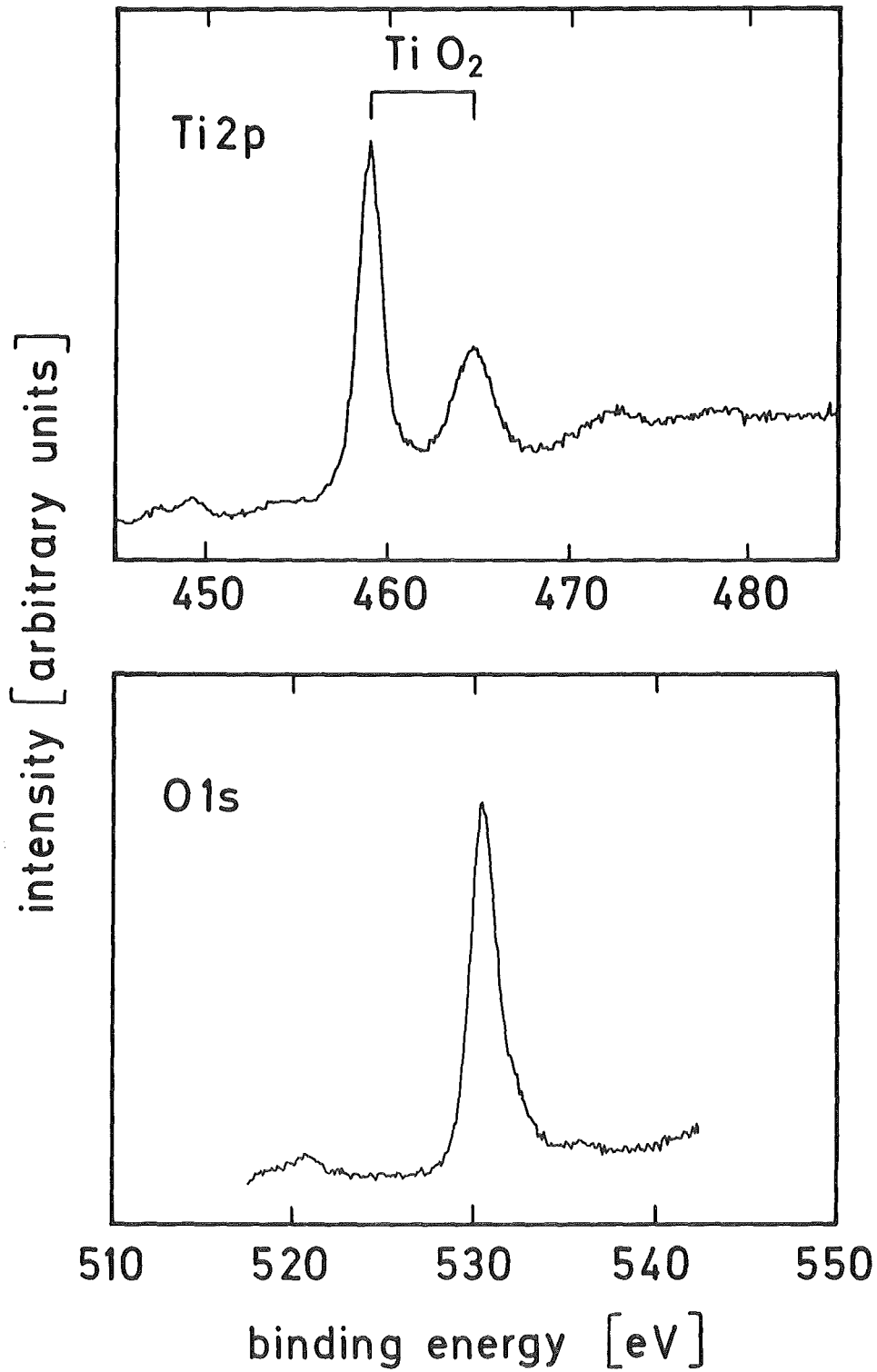


Fig. 15

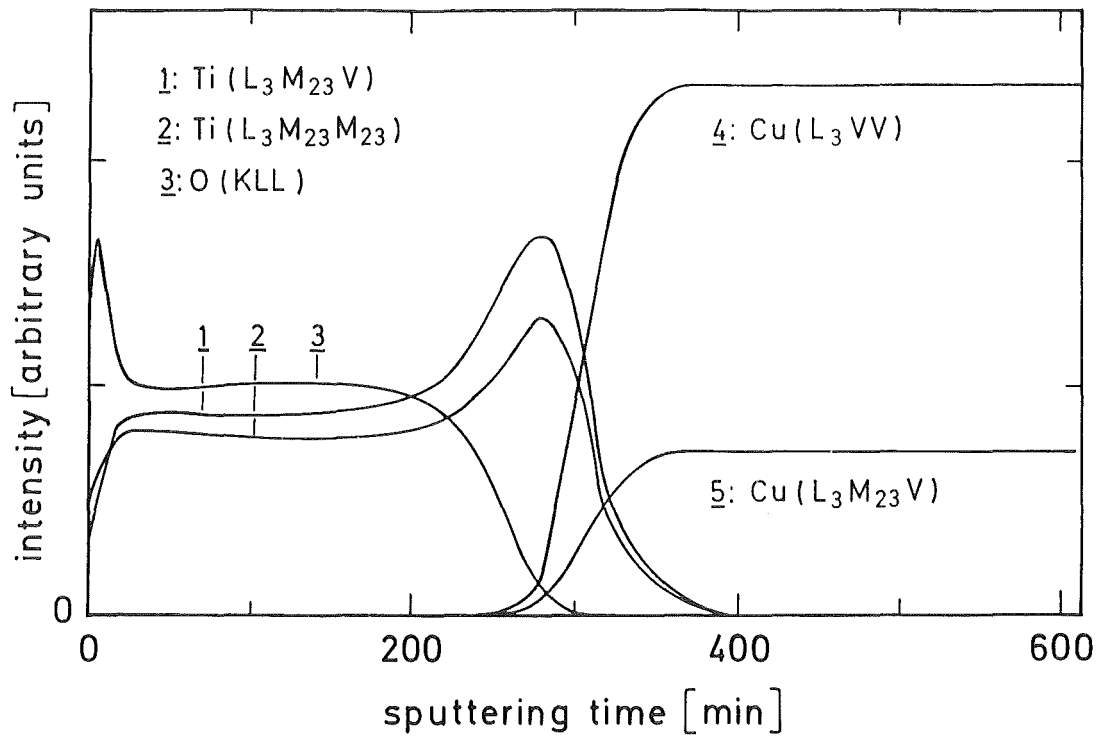


Fig. 16

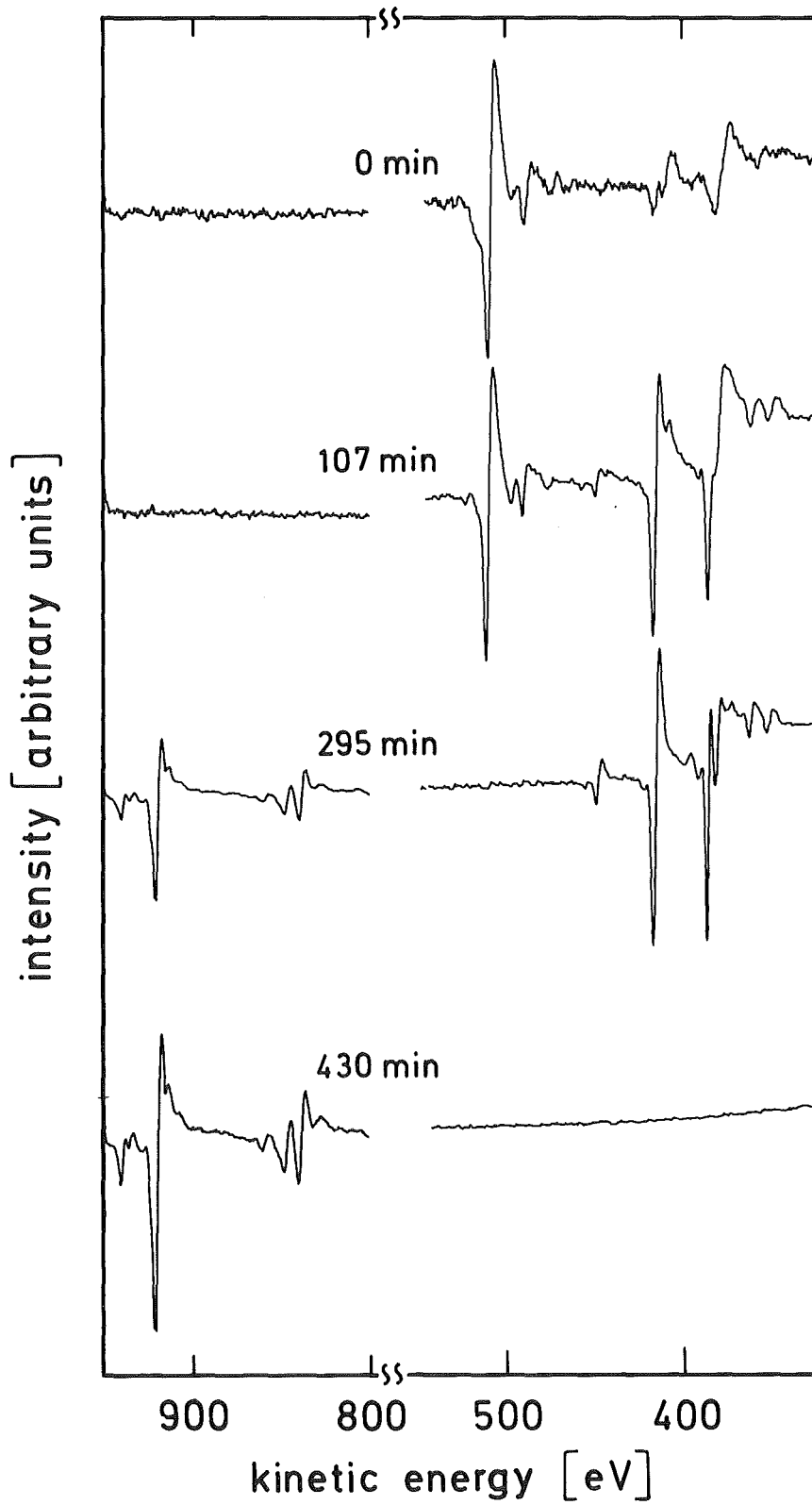


Fig. 17

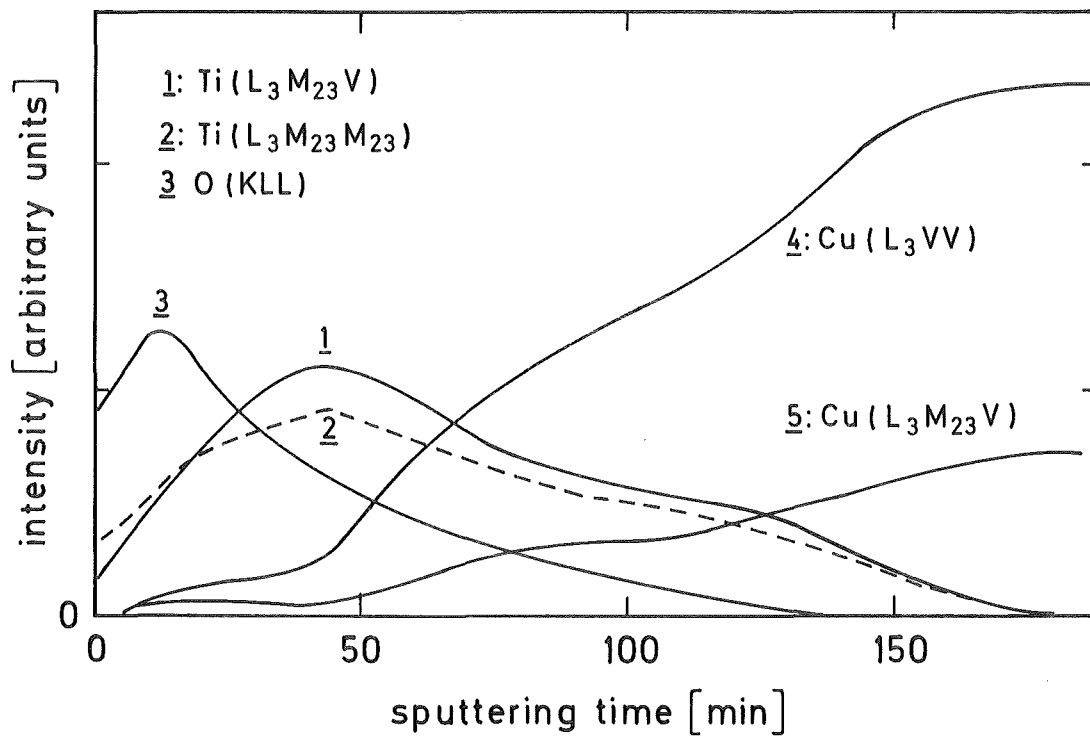


Fig. 18

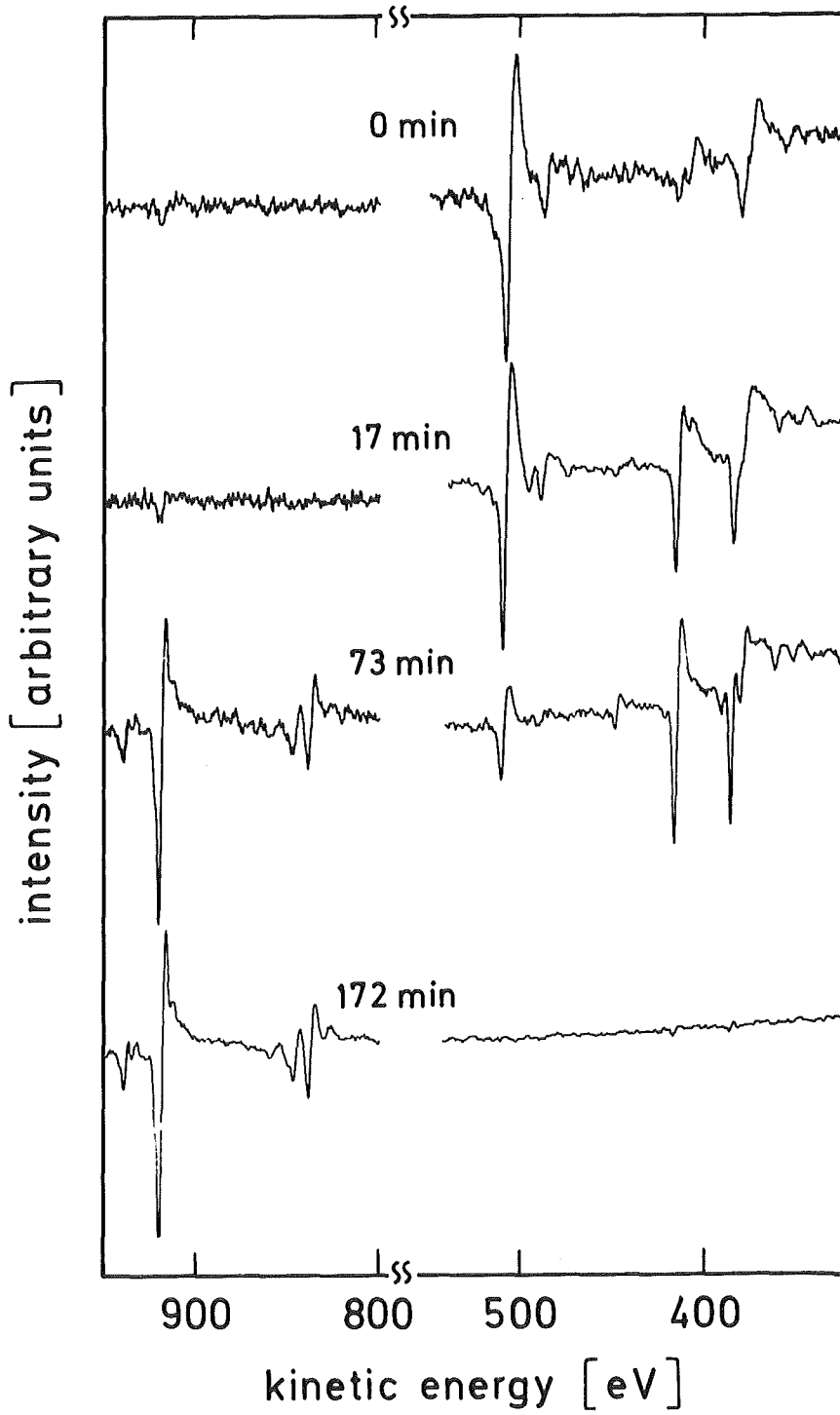


Fig. 19

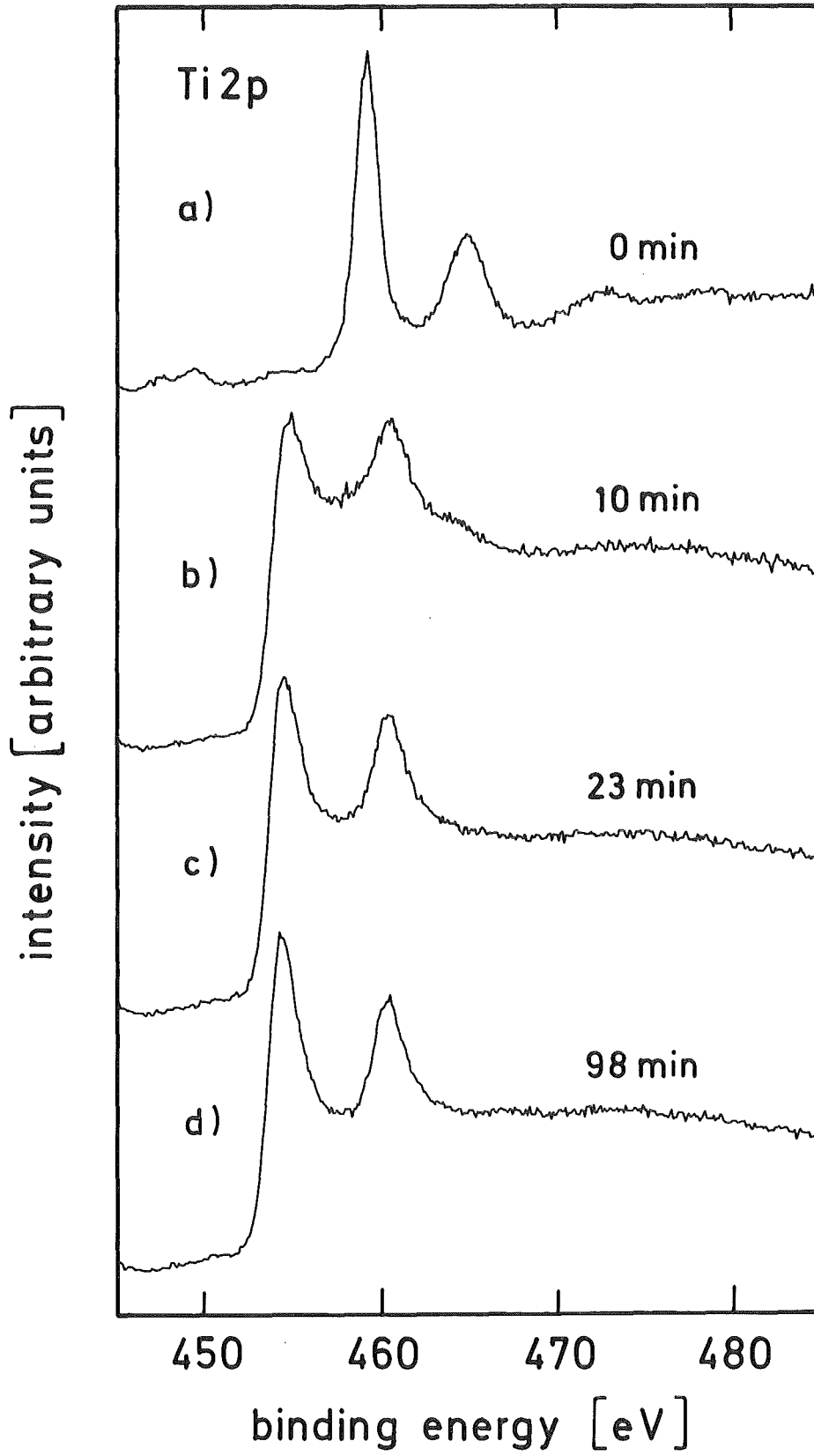


Fig. 20

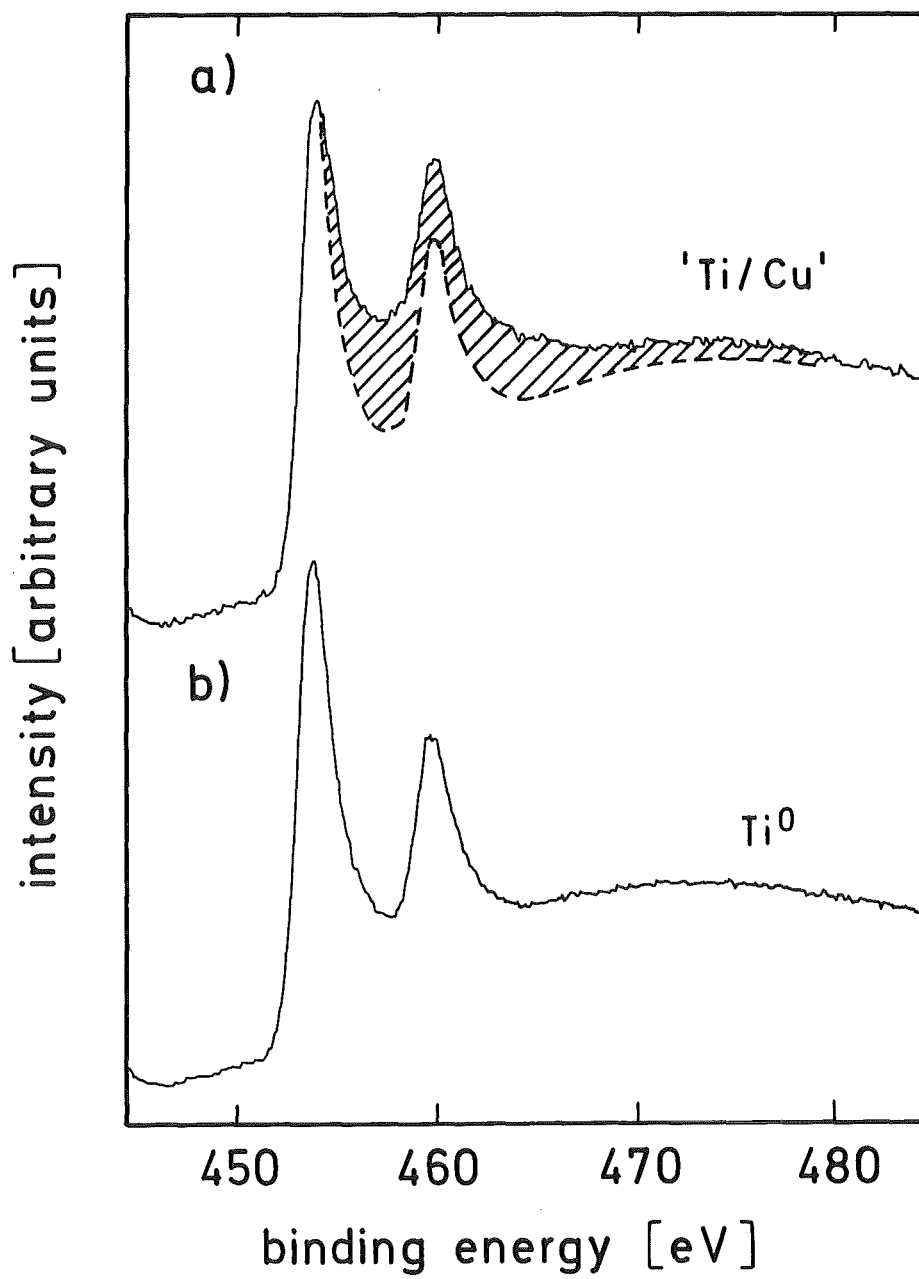


Fig. 21

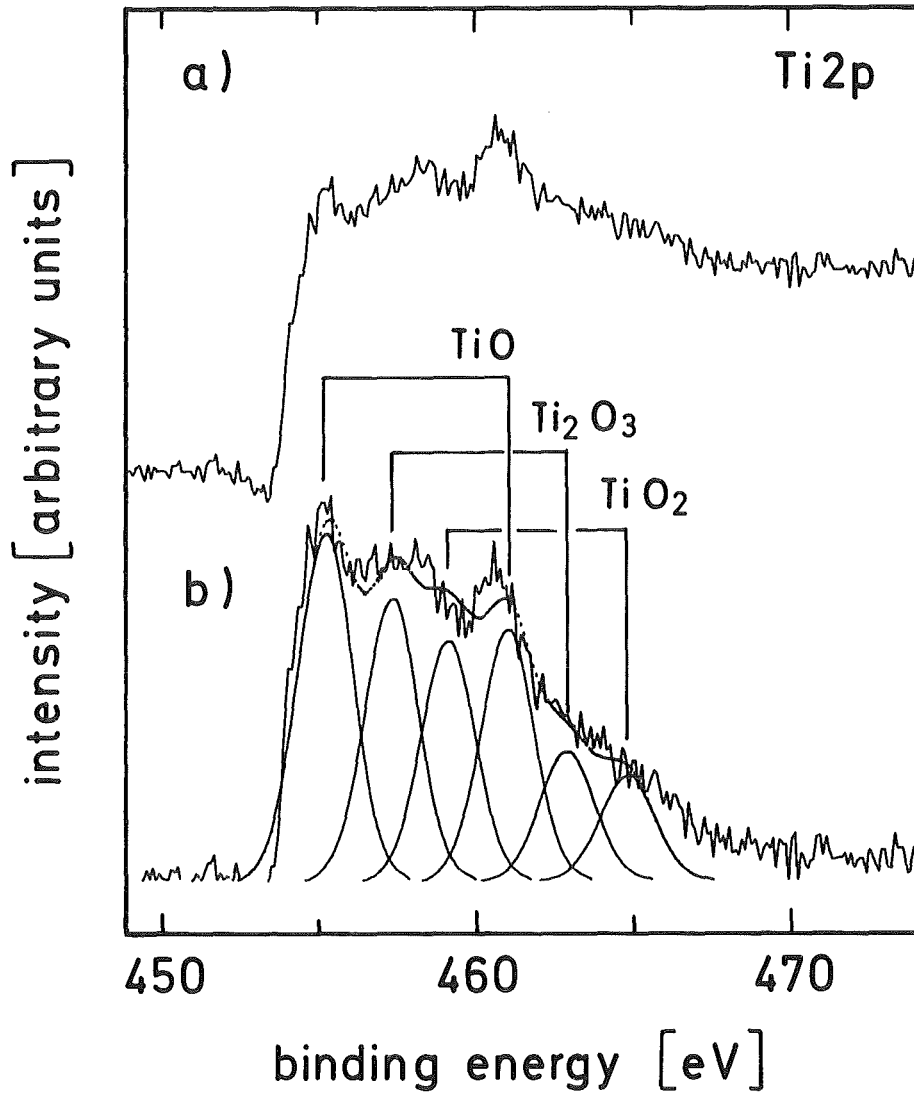


Fig. 22

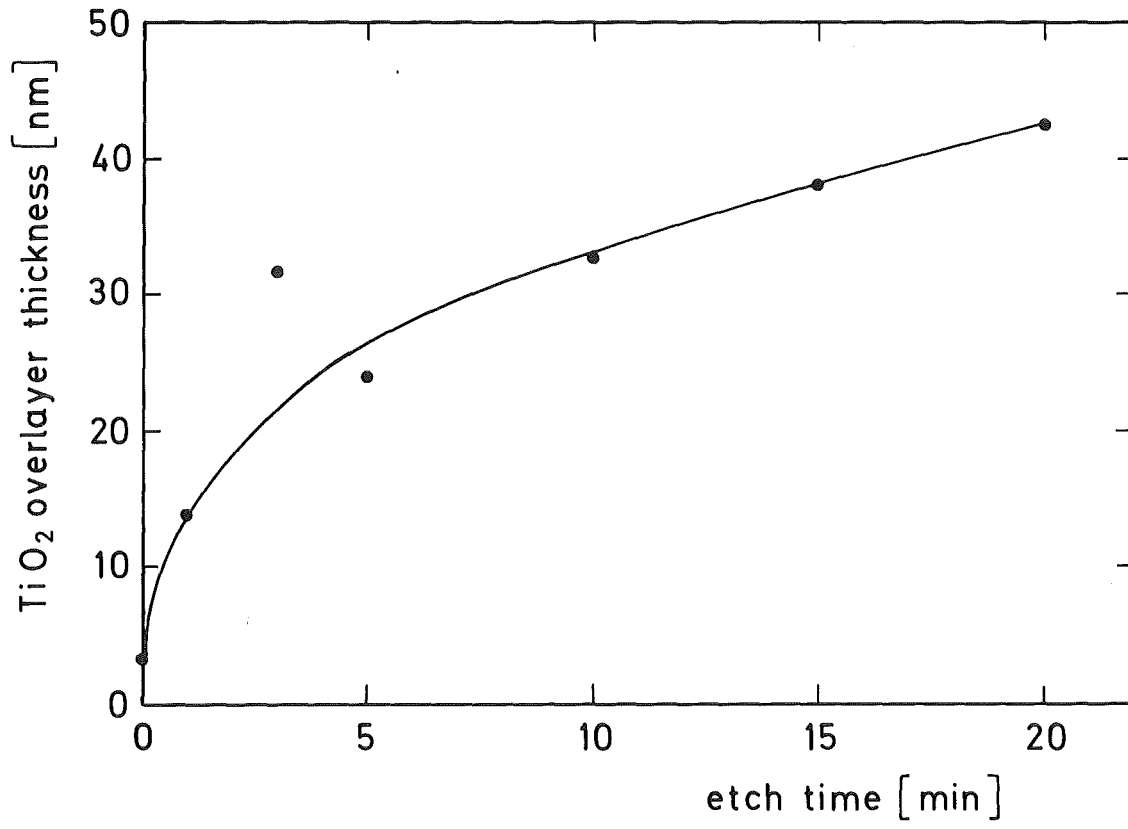


Fig. 23

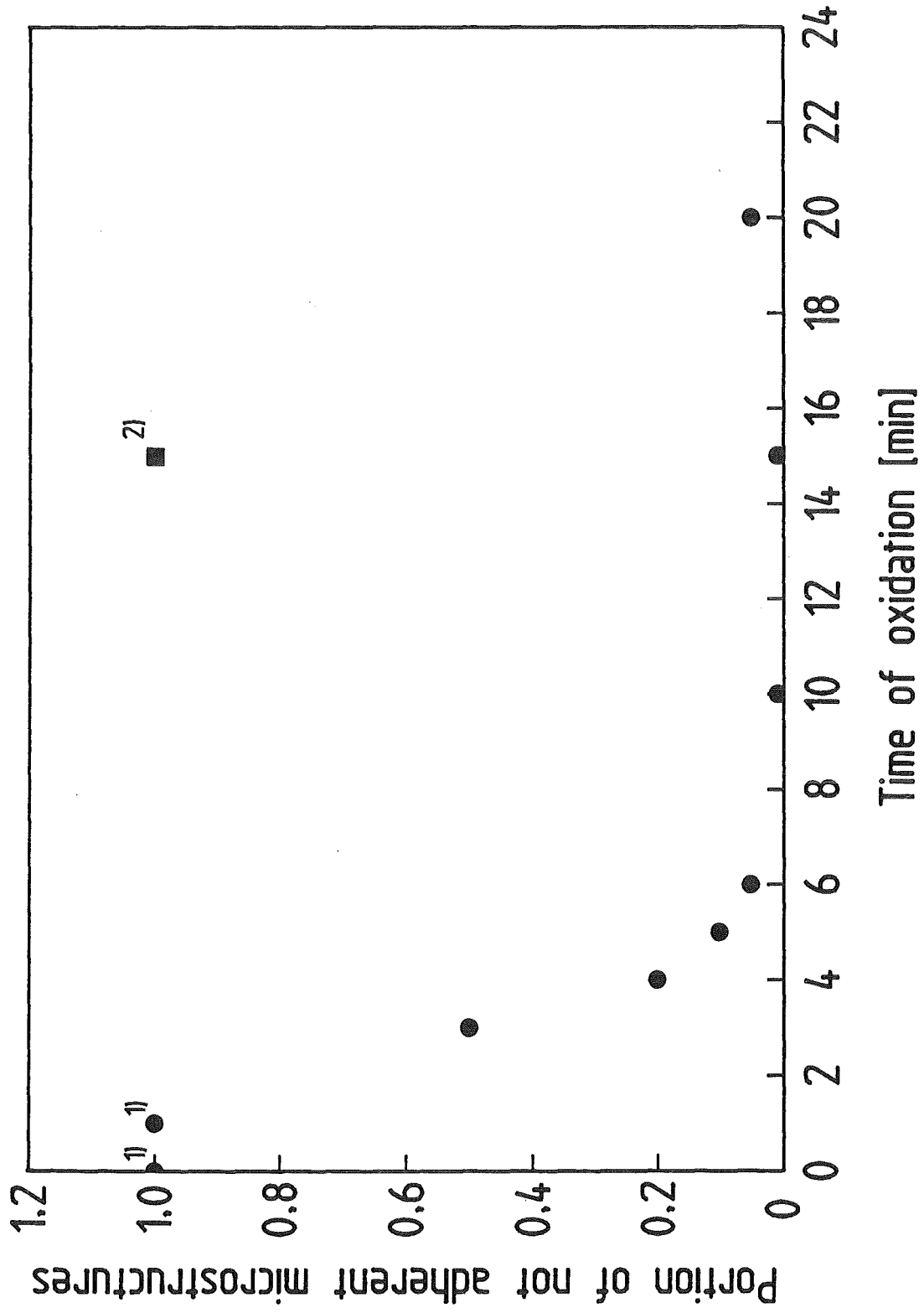


Fig. 24